*Journal of Materials Science Research and Reviews*

*2(1): 42-66, 2019; Article no.JMSRR.46033*

# Review on Oxide Bonded Porous SiC Ceramics: Processing, Properties and Applications

**Dulal Das[1] and Nijhuma Kayal[1*]**

*[1]Central Glass and Ceramic Research Institute, CSIR, 196, Raja S. C. Mullick Road, Kolkata-700 032, India.*

***Authors' contributions***

*This work was carried out in collaboration between both authors. Both authors read and approved the final manuscript.*

***Article Information***

DOI: 10.9734/JMSRR/2019/46033
Editor(s):
(1) Dr. Anjanapura V Raghu, Professor, Department of Basic Science, Centre for Emerging Technology, Jain Global Campus, Jain University, India.
Reviewers:
(1) Yuan-Tsung Chen, National Yunlin University of Science and Technology, Taiwan.
(2) Ahmad Adlie Shamsuri, Universiti Putra Malaysia, Malaysia.
Complete Peer review History: http://www.sciencedomain.org/review-history/27940

***Review Article***

***Received 09 October 2018***
***Accepted 12 December 2018***
***Published 24 December 2018***

## ABSTRACT

Recently the use of porous SiC ceramics is increasing tremendously for various industrial applications due to its excellent properties. Various processing techniques are tried to develop porous SiC ceramics. The fabrication of porous SiC ceramics by an oxidation bonding technique offers several advantages like good oxidation resistance because of air sintering of the ceramics, low sintering temperature, cost effectiveness and easy control over the porosity and other properties of the resultant ceramics. This review deals with processing strategies of oxidation bonding technique. The effect of pore former, powder size, sintering temperature and sintering additives on the properties of the oxide bonded porous SiC ceramics are discussed in detail. The available literatures are thoroughly reviewed with emphasis on mechanical properties, thermal shock resistance properties, gas permeability behavior and separation of particulate from off gas. This review has also enlightened future scope on processing of oxide bonded porous SiC and its usage in various applications.

*Keywords: Porous SiC; oxide bond; mechanical properties; gas permeabilty; thermal shock resistance.*

**Corresponding author: Email: nijhuma@cgcri.res.in;*

## 1. INTRODUCTION

Currently, porous SiC ceramics have been a focus of interesting research in the field of porous materials due to their excellent structural properties, high strength, high hardness, and superb mechanical and chemical stabilities, particularly at high temperatures and hostile atmospheres. Hence porous SiC ceramics have been considered as an ideal candidate for catalyst supports, thermal insulators, high temperature structural materials, kiln furniture, seal pumps for automotive water pumps, composite armour protection, heat exchangers, bio-implants, bearings, abrasion-resistant components such as blast nozzles and centrifuge tiles, burner technology, furnace heating elements, medical implants (hip replacement, orthopedic implants) hydrogen-permselective membranes and hot gas particulate filtration in different industrial processes like integrated gasification combined cycle (IGCC) and coal combustion [1-21]. The use of porous SiC ceramics for hot gas filtration in the coal gasification process especially for pressurized fluidized bed combustion (PFBC) and integrated gasification combined cycle (IGCC) is increasing in order to limit the emission of some corrosive or toxic particles into the environment. For such applications, the ceramic filters must be able not only to resist the chemical attack at high temperature (600 – 900°C) and high pressure (6 – 10 atm) by a variety of gases such as $O_2$, HCl, $H_2S$, $Cl_2$, $SO_2$, NO and $H_2O$, but also to withstand the mechanical stress or thermal shock in the pulse cleaning process [22-24]. There are mainly four methodology developed for manufacturing of porous SiC ceramics: replication, reaction bonding, partial sintering, and expandable microspheres [25-40]. Among them, the reaction bonding technique is a promising method, which involves carbothermal reduction techniques, silicizing techniques [28-29], etc. The processing of porous ceramics using preceramic polymers is another promising route for making porous SiC ceramics [30-37]. Synthesis of hierarchical porous materials from biological templates by carbothermal reduction techniques continues to generate significant interest because biological structures exhibit excellent strength at low density, high stiffness and elasticity, and high damage tolerance integrated into these structures through the evolutionary process [38-40]. All the above mentioned process required high sintering temperature and costly environment which enhance the processing cost. Clay bonded SiC filter has been successfully operated at temperature 620-845°C in an oxidizing atmosphere for 5855 h [22-24]. But they suffer from several disadvantages like (i) Failure due to softening of the bond during service and corrosion, (ii) bond depletion, (iii) bond destabilization, (iv) cracking/spalling due to mismatch of thermal expansion coefficient, etc. Therefore clay bonded SiC filters damaged during long term operation at higher temperature. It is expected that such a problem would not arise for self bonded SiC ceramics [41-42]. Unfortunately, submicron powders and high temperature are required for production. Moreover oxidation remains another problem for high temperature operation of self bonded SiC filters in an oxidizing atmosphere [43-44]. In order to realize low temperature fabrication of porous SiC ceramics, secondary bond phase was considered to bond SiC particles. Utilizing the oxidation derived silica to bond SiC particles, Zhu and co-workers prepared SiC reticulated porous ceramics [45]. Following this, She et al. developed unique oxidation bonding technique for fabrication of porous SiC ceramics with superior oxidation resistance [46-49]. The key feature of the process is that SiC powder compacts are heated in air instead of an inert atmosphere. At the heating stage, surface of SiC get oxidized and SiC particles bonded each other by oxidation derived $SiO_2$ glass, which crystallize to cristobalite at temperature above 1300°C. The technique is referred as oxidation bonding technique. Following this technique various oxide bonded porous SiC ceramics are prepared and characterized [50-101]. The oxidation bonding process is characterized by a low processing temperature and a short sintering time, and is suitable for the preparation of large-size and complex-shaped components. In comparison with the porous SiC prepared by other methods, oxide-bonded porous SiC retains its strength up to very high temperatures and has excellent thermal stability [49]. This method has several advantages compared to the porous SiC ceramics fabricated by other processing techniques. The advantages includes (1) good oxidation resistance because of air sintering of the ceramics (2) low sintering temperature (3) cost effectiveness of raw materials because of coarse staring SiC powders. However, the main drawback of this powder processing route is the agglomeration of the sintering additive and poor dispersion of pore former in the starting materials, which degrades the mechanical and physical properties of the porous ceramics. To avoid these problems colloidal processing route was used to prepare porous SiC ceramics [59].

Sol-gel processing is considered as an alternative approach to fabricate ceramic composites owing to its advantages, such as fine-scale mixing between bond phase additives with ceramic particles and lower processing temperature. Inorganic sol was considered as an effective dispersant for ceramic powders hence enhanced stability of ceramic suspensions by changing their surface potential and also provide high bond strength to ceramic bodies due to the formation of its solid gel at low temperature [96-100]. The addition of a sintering additive via the sol-gel route and a pore former by in situ polymerization was considered as an appropriate choice to overcome the inhomogeniety of the starting particles and expected to enhance and control the properties of the final ceramics. Ebrahimpour et al. used this combination of sol-gel and in-situ polymerization techniques to fabricate a porous ceramic with the desired filtration properties and oxidation resistant properties [74-77]. Traditional colloidal powder processing methods, are often time consuming, requires careful control over the suspension rheology. Assuming that the porosity of the starting compact is uniformly distributed, an infiltration technique was considered to distribute the secondary oxide bond phase homogenously into the final ceramics with negligible shrinkage and without any crack. Recently an infiltration technique is used for fabrication of oxide bonded porous SiC ceramics in which liquid precursor of secondary bond phase is infiltrated into the porous powder compact of SiC followed by heat treatment [86-88,92-94]. Extensive research work has been carried out to fabricate a wide range of porous SiC ceramics by employing various processing methods. However very limited information about the permeability of porous ceramics are available in the literature [57,81,84,90-91]. Particularly, there have been even less attention to the gas permeability behaviour of porous SiC ceramics with the micrometric pore size [101-110].

The application of SiC membranes for water cleaning and liquid separation processes has received recent attention of the scientific community. It has been proved that SiC microfiltration membranes are extremely suitable for filtration of back wash water, surface water and produced water from oil and gas industries [111-121]. Hagen et al. compared silicon carbide membranes with polymeric membranes for particle removal of prefloculated and prefiltered dam water in pilot scale [112]. The SiC dead-end filters are used for pool water filtration in public swimming pools [113]. In addition to dead-end filters, tubular cross-flow filters which are especially interesting for filtration of water with high solid loadings, e.g. industrial wastewater or produced water from oil and gas exploration [114,116-118]. It is reported [117] that the SiC membranes have high thermal (up to 800) and chemical (pH 0 - 14), stabilities and they also have very high permeate flux due to high porosity (about 45%). Saint –Gobain's made R-SiC membranes have been demonstrated [118] to effectively clean water from various sources (i) ground water containing As (ii) municipal swimming pool water (iii) produced water from oil and gas exploration. SiC membranes used for such application are mainly fabricated by ceramically–bonded silicon carbide (CSiC), recrystallised silicon carbide (RSiC) or by reaction-bonded silicon carbide (RBSiC). In all these methods SiC is sintered at high temperature with expensive atmosphere and delicate instrumentation and hence the methods are costly. In order to avoid such problems oxide bonding technique is considered as a simple technique for fabrication of macoporous SiC membrane. Very recently S.C. Kim et al. reported fabrication of oxide bonded SiC microfiltration membrane, in which either clay or glass frit are used as bond phase additives [119-120].The literature review indicate that OBSC ceramics have huge potential in air and liquid filtration application.

The objective of this article is to present an overview on processing and properties of porous SiC ceramics by oxidation bonding technique. The effect of processing parameters on the microstructure, porosity, mechanical, thermal shock resistance, oxidation resistance properties, air permeability and particulate filtration characteristics are discussed. Finally, we suggest unresolved issues that should be addressed for future advances in this field.

## 2. EXPERIMENTAL

Oxidation bonding technique is an unique process for fabrication of porous SiC ceramics at low temperature. Several steps were used, these includes i) powder mixing, ii) pressing/shape making iii) pore former removal and iv) sintering. In the fabrication process commercial SiC powders of variable particle size from submicron to micron size were mixed well with or without pore former ( graphite, starch, PMMA, etc) with or without additives ($Al_2O_3$, MgO, etc) and with or without other oxides ($Y_2O_3$, $Sc_2O_3$, SrO, $CeO_2$,

etc) and pressed at a varying pressure of 23-90 MPa. The powder compacts were than heat treated at temperatures ranging from 1100-1600°C in air with hold time 1-4 h. The main composition of raw materials and processing conditions used in the formation of oxide bonded porous SiC ceramics and their material, mechanical properties are summarized in the Table 1. However, the main drawback of this powder processing route is the agglomeration of the sintering additive and poor dispersion of pore former in the starting materials, which degrades the mechanical and physical properties of the porous ceramics. Therefore Ebrahimpour et al. used combination of sol-gel and in-situ polymerization techniques with a reaction bonding process to develop mullite-bonded porous SiC ceramics. Sol-gel processing is a well-known method to fabricate ceramic composite due to the low cost and high homogenous mixing. In addition, in-situ polymerization is a promising technique to synthesize organic-inorganic composites with enhanced mechanical properties. This method was used to fabricate a porous ceramic with the desired filtration and oxidation resistant properties [74-76]. In this method, SiC particles and calcined alumina powders were coated by alumina sol subsequently; polyethylene was layered on particles using in situ polymerization. By heating the green body, polyethylene was removed as a result of the reaction of the polymer with oxygen and consequently pores were created. Mullite was formed by the reaction between alumina and silica derived from SiC during the sintering process to bond SiC particles together.

To achieve significant performance enhancements, good dispersion of the sintering additive as well as pore former into the starting materials are required. Assuming that the porosity of the starting compact is uniformly distributed, an infiltration technique should result in homogenous formation of a secondary oxide bond phase with the possibility of producing a crack free final ceramics with reduced or negligible shrinkage. Inspired by these possibilities a systematic investigations was carried out on the incorporation of oxide bond precursors into SiC powder compacts by an infiltration based technique. The oxide bond phases that are used include (a) mullite, (b) cordierite and (c) yttrium aluminium garnet (YAG) (d) silica [86-88,92-94]. The reasons behind selection of these bond phase systems are their useful properties ~ high refractoriness, low oxygen diffusion coefficient, low thermal expansion coefficient, low dielectric constant, etc. Other important properties are: high strength that can be retained up to a very high temperature, good thermal and chemical stability, in addition having possibility of synthesizing these materials at low temperatures. α-SiC powders of different grit sizes with or without pore formers were mixed in a acetone medium and the mixtures were ball milled for 24 hrs for homogeneous mixing. The powder mixture was dried in air followed by further drying at 60°C for 24 h. The dry powder mixtures was mixed with 15 wt% solution of polyvinyl alcohol which was used as adhesive, then pressed in a hydraulic pressing at 23 MPa gauge pressure to produce rectangular bar samples. The pressed samples dried at 100°C and subsequently heat treated at 1100°C in air medium for 4 h to obtain porous SiC structure with sufficient handling strength after removal of pore former. Porous SiC compacts were kept into an evacuator and and kept for two hours under the evacuated condition. The precursor sol was added through an inlet which was directed to disperse the sol into the porous compacts under the high capillary action of pores of bulk SiC compacts. After sol incorporation the samples were taken out from the sol and kept for dry under RT and then at 100°C for 24 hours. During this step, the incorporated sol was transformed into gel state due to evaporation of solvent part. Infiltration technique was repeated for several times until the weight gain of sol-gel incorporated porous SiC compacts became constant. The final saturated sol-gel incorporated SiC compacts were sintered at 1300-1500°C to obtain porous SiC ceramics bonded by secondary oxide bond phases.

In another approach mullite- and YAG- bonded porous SiC ceramics was also prepared using sol-gel coated or co-precipitated method. SiC powder suspension was prepared by dispersing a fixed wt% of SiC powders in de-ionized (DI) water followed by ultra-sonication for 30 minutes. Secondary bond phases in the form of sol precursor were added to the SiC powder suspension, the colloidal mixture was stirred for another one hour. The amount of bond phase precursor sol was adjusted in such to yield a definite wt% of secondary bond phase in the final ceramics. The SiC powders dispersed in mullite sol maintained at *p*H~2 and at 7 to obtain mullite coated SiC powder and SiC co-precipitated with mullite respectively. The SiC powders dispersed in YAG sol was maintained at *p*H~9 by adding 1 (N) solution of ammonia to obtain precipitation of

colloidal particles of YAG on the surface of SiC particles. The coated and co-precipitated powders were filtered, washed four times with DI water and dried at 100°C for 24 hour. The dry powders were then calcined at a particular temperature to remove volatile components. The calcined coated or co-precipitated powders were sieved using sieving net to make uniform powder size and then pressed in bar shape. Fig. 1 shows the schematic processing of porous SiC ceramics by sol-gel coating method. The bar samples were dried at 100°C for 24 hours and finally sintered at 1300°C for mullite system and at 1450°C for YAG system. Oxide bonded porous SiC ceramics (OBSC) were named as SBSC, MBSC, CBSC and YBSC for silica, mullite, cordierite and YAG as bond phase respectively. The effect of different secondary bond phases on the microstructure of porous SiC ceramics are presented in Fig. 2.

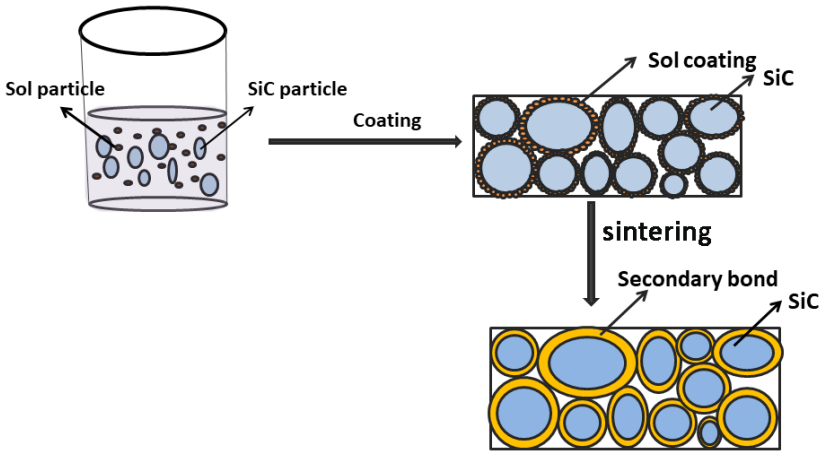


**Fig. 1. Schematic of fabrication porous SiC ceramics by sol-gel coating process**

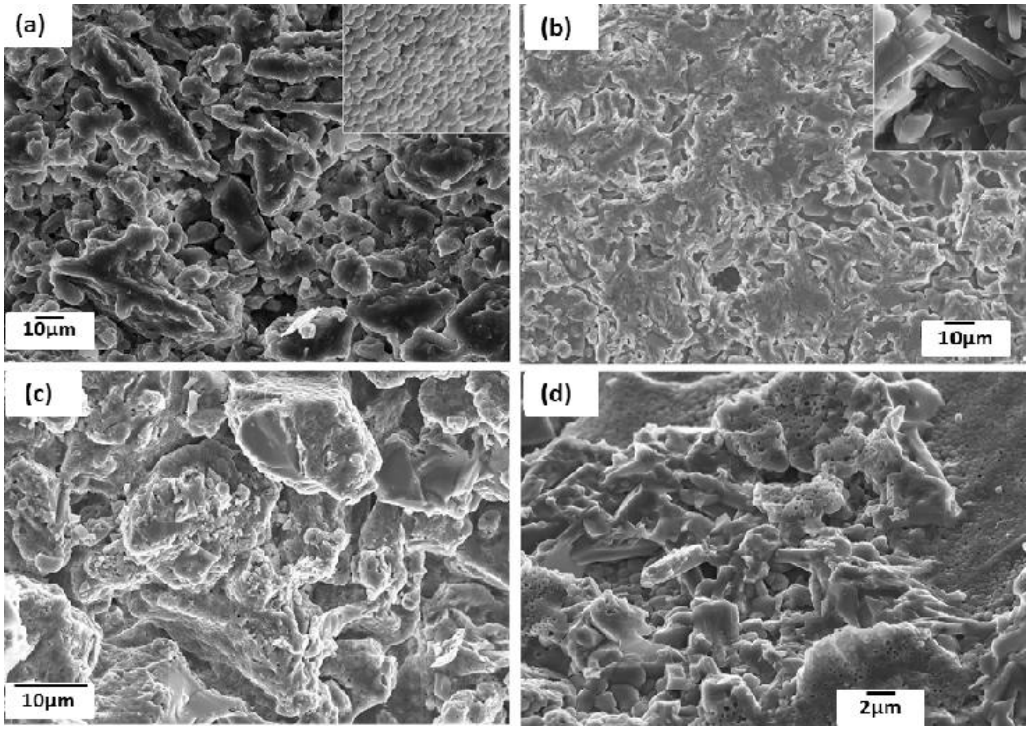


**Fig. 2. Effect of secondary bond phases (a) silica (inset shows fish scale morphology of cristobalite) (b) mullite (inset shows needle shape morphology of mullite) (c) cordierite and (d) YAG on the microstructure of porous SiC ceramics**

**Table 1. Effect of addition of other oxide on material and mechanical properties of porous OBSC ceramics**

| SiC ($d_{50}$ in μm) | Bond type/ [Ref] | Additives ($d_{50}$ in μm) | Pore former | Sintering temperature ($^{o}$C) | Porosity (vol%) | Pore diameter (μm) | Flexural strength (MPa) |
|---|---|---|---|---|---|---|---|
| 0.6-2.3 | Silica [46] | - | - | 1100-1400/1 hr | 28-41 | - | 60-190 |
| 2.3 | Mullite [49] | $Al_2O_3$(0.2) | Graphite (5,10 and 20) | 1450/0.5-21hr | 36-75 | 2.5-12 | 10-52 |
| 0.3 to58 | Silica [49] | - | Graphite (5,10 and 20) | 1450-1500/1-5 hr | 31-36 | 2.5-12 | 40-133 |
| 0.34 | Silica [50] | - | Microbead(20) | 1400/1hr | 40 | 25-30 | 65 |
| 20 | Mullite [51-53] | $Al_2O_3$ (0.6) and $Y_2O_3$ (5.0) | Graphite (10) | 1300-1550/4hr | 34-57 | 1.6-8 (Bimodal) | 5-28 |
| 20 | Cordierite [62] | $Al_2O_3$, talc, clay | Graphite | 1360/2hr | 28-60 | 1.9-4.9 (Bimodal) | 10-55 |
| 10 | Cordierite [60] | $Al_2O_3$, (0.6) MgO | Graphite (5,10, 20) | 1200-1400/2-4hr | 28-66 | 2-8 | 3-71 |
| 10 | Cordierite [63] | $Al_2O_3$, (0.6) MgO, $CeO_2$ | Graphite (10) | 1250-1400/2hr | 28-56 | 2.4-3.2 | 4-36 |
| 10 | Mullite [65] | $Al_2O_3$(0.6) preheat-treated aluminosilicate | Graphite (10) | 1350–1550/ 2 hr | 35-53 | 1.6-4 | 14-87 |
| 90 and **0.5** | Mullite [66] | $Al_2O_3$, (0.4) MgO, CaO, SrO | C template (20) | 1450/2 | 44-49 | - | 6-44 Superior st, SrO |
| 65 and **0.5** | Mullite [67] | Al, ALN, $Al_2O_3$, $Al(OH)_3$ | - | 1450-1500/1-2 hr | 35-46 | - | 5-19kNm/kg |
| 65 | [72] | $Al(OH)_3$ | - | 1450-1500/1-2 hr | 46-54 | - | 3-14 |
| 65, 0.7 | SiC bonded [70] | Si (1) | Carbon black | 1700-1800/1 hr in Argon | 38-46 | 5-25 | 3-42 |
| 20 | SiC-cordierite composite [55] | Clay, talc, alumina | Graphite | 1200-1400/2 hr | 27-60 | - | 9.3-54.6-26 |
| 10 | Sodium borate [73] | $Na_2B_4O_7$ | Starch | 650-800/30 min | 47-64 | 15-25 | 3-37 |
| 2.4 | Mullite [78] | Porous Alumina column (37.3) | Graphite (18.7) | 1300-1500/3hr | 30-47 | - | 22-56 |
| 23 | Cordierite-mullite [80] | $Al_2O_3$(11.7) MgO, | Graphite (18.7) | 1300-1450/3hr | 18-50 | 2.98 | 13-64 |
| 125-7 | Glass [81] | Glass (61 wt.% $SiO_2$, 24% $Al_2O_3$, 5% CaO, 2%$Na_2$ O, 2% $K_2O$, and 6% other materials) | - | 850/1hr | 32-65 | 6-127 | - |
| 22.8 | Cordierite [82] | Diatomite (4.2) Talc (2.6) $Al_2O_3$ (27.3) | Graphite (18.7) | 1150-1400/3-7 hr | 27-46 | 3 | 25-65 |
| 22.4 | Silica [85,90] | Silica sol (with and without) | - | 1300/4hr | 26-36 | 5-7 | 29-48 |
| 22.4 | mullite [86] | $Al_2O_3$ and Silica Only $Al_2O_3$(6.5) | -Petroleum coke (11) | 1500/4hr 1500/4hr | 30 29-56 | 5 6-9 | 47 9-34 |
| 22.4 | Cordierite [91] | $Al_2O_3$(6.5) MgO, | Petroleum coke (11) | 1350/4hr | 32-68 | 6-50 | 5-54 |
| 4.5-99 | Mullite [87-88] | Mullite sol | Graphite (12) | 1300-1500/4 hr | 31-48 | 2-30 | 16-49 |
| 22.4, 53, 99 | Cordierite [93-94] | Cordierite sol | Graphite (12) Microbead (8,50) | 1300-1400/3 hr | 30-49 | 4-22 | 13-38 |
| 22.4, 53 99 | yttrium aluminum garnet (YAG) [92] | YAG sol | Graphite (12) Microbead (8,50) | 1300-1500/3 hr | 29-41 | 5-30 | 8-41 |

*Microbead = poly(methyl methacrylate-co-ethylene glycol dimethacrylate)*

## 3 RESULTS AND DISCUSSION

### 3.1 Mechanism of Bond Formation

SiC oxidizes during thermal heating with the formation oxides of silicon. Depending on the oxygen potential this oxidation may be active with the formation of SiO or, passive with the formation of $SiO_2$ [122-123]

$$SiC + O_2 = SiO + CO_2 \quad (1)$$

$$SiC + O_2 = SiO_2 + CO_2 \quad (2)$$

The active oxidation is associated with a critically low partial pressure of oxygen, where as adequate supply of oxygen at the reaction front ensures passive oxidation with the formation of protective $SiO_2$ scale and gain in weight. This $SiO_2$ may be vitreous at the formation temperature which under suitable heat treatment conditions devitrifies to the cristobalite phase. In a porous body the percolation threshold for permeation of molecular oxygen is around 16-22 vol.% [124-125]. If the porosity can be maintained above this percolation threshold limit, molecular oxygen permeates to oxidize SiC particles with the formation of $SiO_2$. The silica scale under controlled heat treatment conditions converted to cristobalite that join the neighbouring SiC particles as shown in Fig. 2a. Cristobalite with fish-scale morphology was observed in the microstructure which was also observed in silica bricks [126-127]. The cristobalite has the characteristic fish-scale morphology arises from the grain boundaries of the original quartz grains [126]. Oxides like alumina, magnesia, etc., were mixed with starting SiC powder for the formation of other oxide bond like mullite, cordierite at low temperature which led to change in material and mechanical properties. In presence of $Al_2O_3$, there is a strong thermodynamic possibility of formation of mullite (CTE= 5.4 x $10^{-6}/^oC$) which has nearly matching coefficient of thermal expansion with SiC (CTE = 4.7 x $10^{-6}/^oC$) .The oxidation derived $SiO_2$ reacts with alumina to form mullite at a temperature over $1410^oC$. The mullitization between $SiO_2$ and α- $Al_2O_3$ is explained by solution precipitation mechanism. $SiO_2$ does not form a viscous liquid phase at $1400^oC$ but shows a viscous softening. Due to the superfacial softening, the α-$Al_2O_3$ particles penetrate into viscous $SiO_2$ glass, leading to the nucleation of mullite. At 1450°C, the viscosity of $SiO_2$ glass decreases and more $Al^{3+}$ ions gets dissolved into viscous $SiO_2$ glass. Above $1500^oC$, the mullite formation occurs by the reaction between cristobalite and α- $Al_2O_3$. Because of short diffusion distances achieved by the viscous flow assisted sintering, the rate of mullitization is accelerated drastically [128-129]. Formation of mullite during sintering of porous SiC is described by following equations.

$$SiC + 2O_2 \rightarrow SiO_2\left(amorphous\right) + CO_2 \quad (3)$$

$$AmorphousSiO_2 \rightarrow Cristobalite \quad (4)$$

$$3Al_2O_3 + 2SiO_2 \rightarrow 3Al_2O_3.2SiO_2\left(mullite\right) \quad (5)$$

After enough mullite is formed, the interfaces of $SiO_2$-mullite and $Al_2O_3$ –mullite appear. $SiO_2$ and α- $Al_2O_3$ inter-diffuse across the mullite layer and the formation of mullite is diffusion controlled [129]. It has been proved that with increasing amount of alumina open porosity decreases, and the flexural strength increases significantly. Sintering at 1300°C or above resulted in the formation of needle shaped mullite phase between the SiC particles at the contacting points as shown in Fig. 2b. The needle shaped morphology of mullite phase has been reported by several researchers [130-131] The mullite bond phase was seen to be of ~2-4 μm in width and 20-40 μm in length in the ceramics prepared by infiltration of mullite precursor sol [91]. Lee et al. obtained needle-like mullite phase of 1 - 2 μm in length and 0.1 - 0.3 μm in width by sintering at 1300°C for 2 hours; the length and width of the mullite phase had grown to 10 - 20 μm and 1 - 2 μm respectively when the sintering temperature was raised to 1600°C [131]. Average activation energy of mullite was obtained as ~1200-1275 kJ $mol^{-1}$ produced through reaction of powder sample of $Al_2O_3$ and oxidation derived $SiO_2$ from SiC [132].

If MgO is present, there is a possibility of formation of cordierite ($2MgO.2Al_2O_3.5SiO_2$); cordierite may be another important oxide bond phase due to its low thermal expansion coefficient (~1.5 x $10^{-6}/^oC$) and low cost [133-134]. During heat treatment of powder compacts of SiC,$Al_2O_3$ and MgO, silica reacts with MgO and $Al_2O_3$ to form cordierite below$1350^oC$. Sintering of SiC is described by series of reactions as follows:

$$MgO + Al_2O_3 \rightarrow MgO.Al_2O_3\left(spinel\right) \quad (6)$$

$$2MgO + 2Al_2O_3 + 5SiO_2 \rightarrow 2MgO.2Al_2O_3.5SiO_2\left(cordierite\right) \quad (7)$$

$$2(MgO.Al_2O_3) + 5SiO_2 \rightarrow 2MgO.2Al_2O_3.5SiO_2\,(cordierite) \quad (8)$$

The mechanism of formation of cordierite ($Mg_2Al_4Si_5O_{18}$) from mixed oxides is well documented [135-137]. At around 1250°C MgO and $Al_2O_3$ of the spinel dissolves into $SiO_2$ and subsequently turns into α-cordierite (orthorhombic structure) from the solid solution at its limit of solubility. It is reported that reaction between spinel and $SiO_2$ proceeds via the formation of a μ-cordierite phase (a low temperature metastable modification of cordierite with hexagonal structure) as a stuffed derivative of β-quartz phase. From TG-DTA analysis of powder compact of SiC+ $Al_2O_3$ + MgO, Liu et al. observed three exothermic peak at 1255.4, 1292,3 and 1346.7 °C [62]. The peak near 1255.4 °C was explained due to the formation of α-cordierite, which was also confirmed by the phase analysis of the samples sintered at different temperatures. They also found that the increase of $Al_2O_3$ + MgO additions results in more cordierite, spinel and Mg-Al-Si-O glass. Cordierite and spinel can enhance the strength of porous SiC ceramics, but the strength is impaired when excessive Mg-Al-Si-O glass exists in the porous ceramics, because of fragile nature of glass. Microstructure indicated well developed necks formation made of reaction-derived silica and cordierite as shown in Fig. 2c. At higher magnification spherical-, and lethal shaped morphologies are seen and EDS analysis indicated presence of Mg, Al, Si and O elements which supports the cordierite phase formation [93]. The cordierite crystals were found to be 3-5 μm in length and 0.5-1.0 μm in width and spherical shaped cordierite was found be of ~1 μm diameter. Moftah El-Buaishi et al. also observed the spherical shaped cordierite crystals of dimension 1 μm and some agglomerated particles of ~10 μm [138]. For MgO-$Al_2O_3$-$SiO_2$ cordierite-based glasses activation energy crystallization is estimated by many authors and found to vary over a wide range, ~ 270 to 630 kJ $mol^{-1}$ [139-141]. Average activation energy of μ and α phase of cordierite was obtained as 644.22±33.33 and 849.75±24.34 kJ $mol^{-1}$ produced through reaction of powder sample of $Al_2O_3$, MgO and oxidation derived $SiO_2$ from SiC [91]. The micrographs of YAG incorporated ceramics showed fish-scale, spherical-, rod or needle- shaped morphologies for silica, YAM or YAP and $Y_2Si_2O_7$ phases respectively as shown in Fig. 2d.

### 3.2 Effect of Other Additives

In order to lower the sintering temperature of porous SiC ceramics, alkaline earth metal oxides, $Y_2O_3$ has been chosen as sintering additive as they have lower eutectic temperatures $Y_2O_3$– $Al_2O_3$–$SiO_2$ (1360°C), $Sc_2O_3$–$Al_2O_3$–$SiO_2$ (1450°C), MgO–$Al_2O_3$–$SiO_2$ (1355°C) and CaO–$Al_2O_3$–$SiO_2$ (1170°C) SrO–SiO2 (1358°C) [142-145] when $Al_2O_3$ exists, SrO–$Al_2O_3$–$SiO_2$ can form eutectic liquid at lower temperature than 1358°C. Addition of small amount of $Sc_2O_3$ accelerated the rate of solid state diffusion to form a ternary Sc-rich aluminosilicate, resulted enhanced mullite formation at temperatures between 1350 and 1550°C [142]. Choi et al observed that in presence of SrO the flexural strength of MBSC ceramics was improved because the addition of SrO formed a denser strut than the other alkaline earth metal oxides (MgO, CaO) [66]. In the powder processing route the cordierite phase was accompanied by the phase of spinel ($MgO{\cdot}Al_2O_3$), which impaired the thermal shock resistance of porous SiC ceramics due to the high thermal expansion coefficient of spinel. To avoid this problem Liu et al. used $CeO_2$ as sintering aids and observed that with addition of 2.0 wt.% $CeO_2$ a large amount of cordierite but only a trace of spinel at 1250°C. Due to the enhancement of neck growth by the addition of $CeO_2$, the porous SiC ceramics exhibited better mechanical properties than the ceramic prepared without $CeO_2$ [63]. Typical microstructure of mullite bonded porous SiC ceramics with addition of other additives are shown in Fig. 3 which exhibits strong neck formation with connected porous structure.

Fig. 4 shows the XRD pattern of silica-, mullite- and cordierite bonded SiC porous ceramics. For silica bonded porous SiC ceramics the main peaks were due to SiC and cristobalite. In case of mullite bonded porous SiC ceramics SiC, cristobalite, mullite was detected as the major crystalline phases. Similarly for cordierite bonded porous SiC ceramics peaks of cordierite were detected along with major peaks of SiC and cristobalite.

### 3.3 Effects of Particles Size of SiC and Pore Former and on Porosity and Pore Diameter of Final Ceramics

For application of porous ceramics as gas filter, a desired pore size is needed to achieve high particulate filtration efficiency. This can be easily

obtained by oxidation bonding process through incorporation of various pore forming agent like, saw dust, rice husk, starch, yeast, graphite, organic particulates, etc. During heating in air these particulates burn out, leaving pores in the OBSC ceramics. For oxide bonding of porous SiC ceramics polymethylmethacrylate (PMMA; microbeads), sodium bicarbonate, graphite pore formers are commonly used. Chun et al. reported variation of porosity in a range of 19 to 77 vol.% using microbead (of $d_{50}$=20 μm) as pore former in SBSC ceramics simply by the variation of amount of the pore former [50]. Gnesin et al. prepared highly porous SiC ceramics (with porosity up to 70%) by the use of varied amount of sodium bicarbonate pore former [146]. She et al. used SiC particle of size 0.3 μm, observed average pore diameter of 3.4, 5.3 and 7.6 μm on using graphite of particle sizes 5, 10 and 20 μm respectively [48]. They calculated the pore diameter theoretically from the schematic diagram using following equation and the result matched excellently with the experimental results.

Ding et al. noticed change in pore size distribution pattern from monomodal to bimodal with increase of graphite particle size from 5 to 20 μm, with an average pore diameter 1.6 and 8.0 μm [53] respectively. It was explained that since 20.0 μm SiC particles were used, the size of the pore by stacking of SiC particles should be theoretically 8.3 μm, provided that spherical SiC particles are in dense cubic stack. When graphite particles of 5 and 10 μm were used, the sizes of the pore by burning out of graphite closely match with pores by stacking of the SiC particles, so that there is no remarkable difference between them in the average pore diameter. When graphite particle increased to 20 μm, the pores formed by burnout of graphite are much larger than those from stacking of SiC particles; as a result bimodal pore size distribution was obtained. CBSC ceramics showed variation of porosity from 28 to 66 vol% with increase in amount of pore former fraction from 0 to 0.60 prepared from powder mixture containing SiC, $Al_2O_3$, MgO and graphite. It is also reported that with the increase in graphite particle size from 5 to 20 μm pore diameter increased from 1.2 to 7.5 μm but porosity remained almost same on keeping the amount of pore former constant [62]. On the other hand, the pore diameter of OBSC ceramics was found to be strongly dependent on

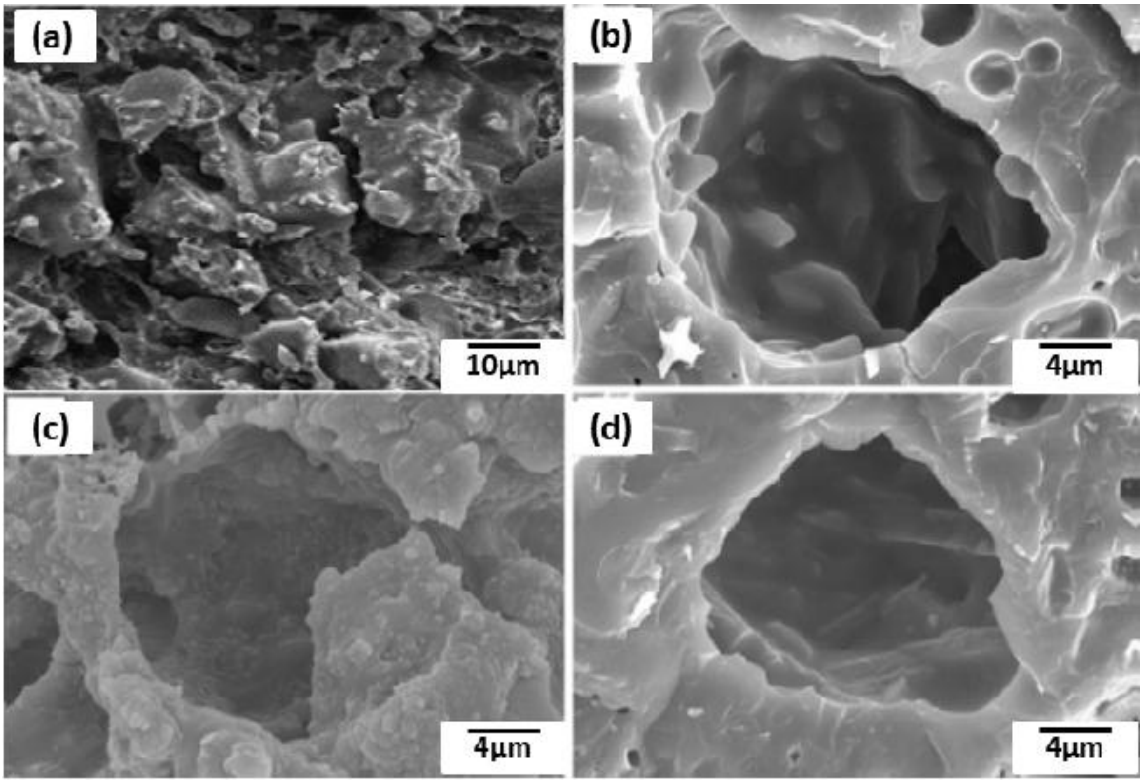


**Fig. 3. Typical SEM micrograph of porous mullite bonded SiC ceramics prepared with (a) 1.5 wt.% $Y_2O_3$ sintered at 1450°C for 4 h [51] (b) 4 wt% MgO (C) 4 wt% CaO and (d) 4 wt% SrO sintered at 1400°C for 2 hr [66]**

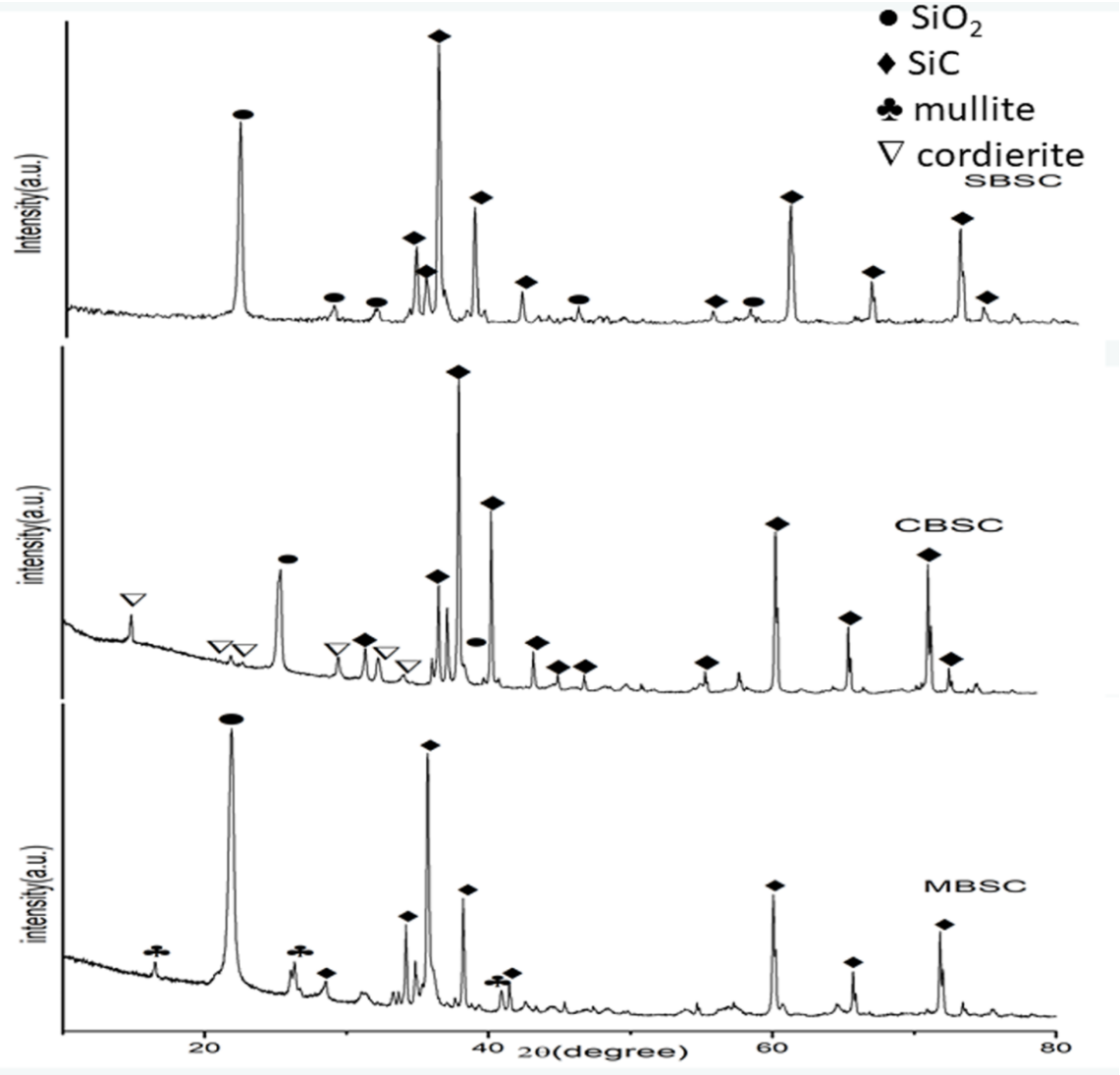


**Fig. 4. XRD pattern of silica-, mullite- and cordierite bonded SiC porous ceramics**

the size of the starting powders. She et al. reported mean pore diameters of 2.5, 3.5, 7.2 and 11.6 μm for the samples prepared using 6-, 10-, 27- and 58-μm SiC powders [49]. Baitalik et reported mean pore diameter of 3.5, 10.6 and 22.3 μm and 4.8, 11.9 and 21.5 μm for the cordierite-infiltrated porous SiC samples prepared using 22, 57 and 99 μm SiC powders sintered at 1300 and 1400 °C respectively [93]. With increase of porosity from 29 to 56%, pore size increased from from 5.5 to 10.6 μm as reported for mullite bonded porous SiC ceramics [90]. Similar observations were made for the cordierite bonded porous SiC ceramics, with increase of porosities from 30.2 to 55% pore size changed from 5.5 to 17.9 □m with further increase of porosity to 55%, the pore size increased to ~49 μm [91].

Eom et al. studied [72] the effect of incorporation of submicron size SiC powder (in addition to the coarse SiC powder) on the microstructure, densities and mechanical properties in case of reaction sintering mullite bonded SiC ceramics. The porosity was increased with increase in amount of pore former due to the increased number of pores as shown in Fig. 5. The average pore diameter did not changed significantly with amount of pore former, but they get changed significantly with changing pore diameter of the starting pore former. Hence, porosity, pore sizes can be controlled by selecting the size, amount and type of pore former, sintering temperature, size of starting SiC powder, sintering additives and bond phases in the final ceramics.

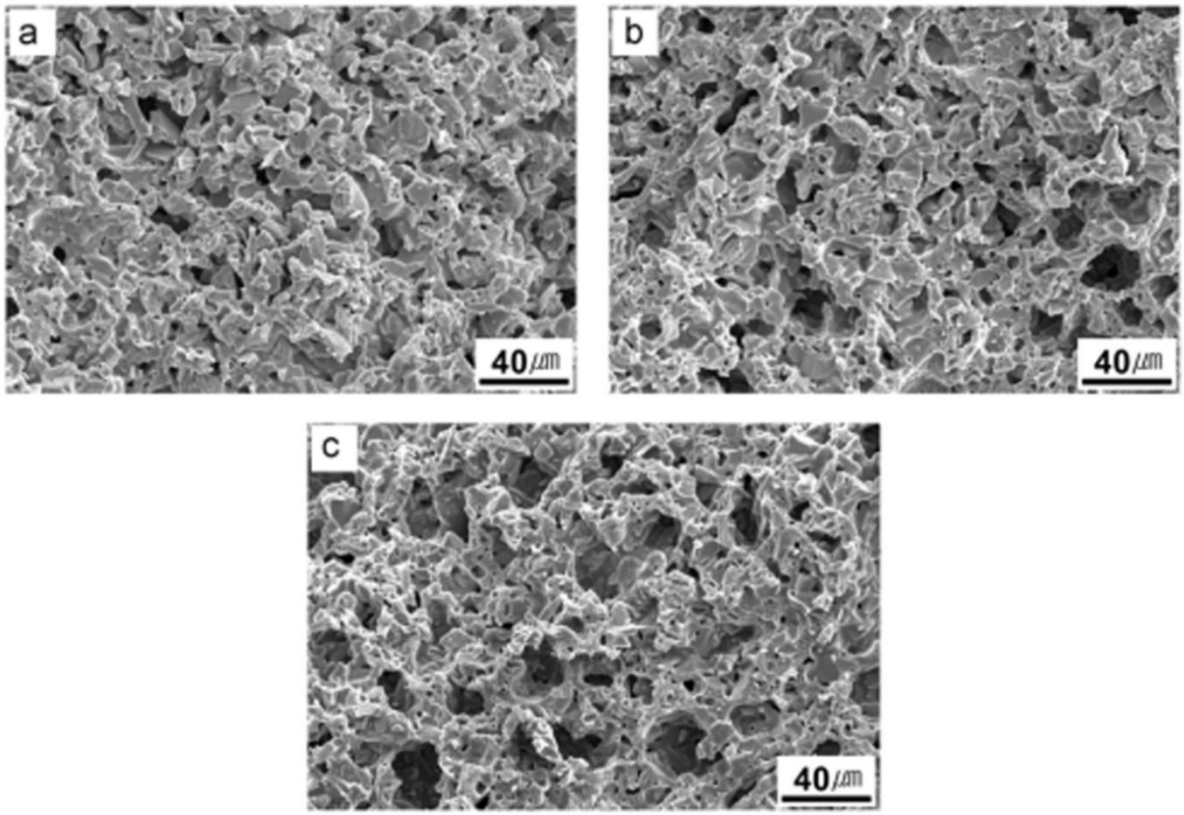


**Fig. 5. Effect of starch content on the microstructure of porous SiC ceramics (a) 40 (b) 43 and (c) 46 wt%. [ 73]**

### 3.4 Effect of Sintering Temperature

Sintering temperature and hold time are other important processing parameter for oxide bonded porous SiC ceramics. The heat treatment temperature has significant effects on % SiC oxidation degree, porosity and pore size distribution of the porous SiC ceramics. A gradual gain in mass was observed at >1000°C in the thermogrametric analysis of the powder mixtures, because of on set oxidation of SiC. Although SiC might began to oxidise at >800°C, it became noticeable only at 1100°C [147]. During sintering of the SiC compact, SiC get oxidized forming silica. The degree of oxidation (f) of SiC can be expressed as [148]:

$$f = 2C_M \times 100 \quad (9)$$

where $C_M = (M_S^{/} - M_S)/ M_S$, $M_S^{/}$ and $M_S$ being the mass of SiC before and after oxidation. The oxidation degree of SiC depends on several factors (i) sintering temperature (ii) particles size of the SiC powder (iii) amount of additives ($Al_2O_3$/ $Al_2O_3$+MgO) (iv) addition of other oxides like $Y_2O_3$, $CeO_2$, alkaline earth metal oxides, etc. It is reported that oxidation degree of SiC rises steeply with increase in sintering temperature and hold time. She et al. observed [43] sharp rise of vol% of $SiO_2$ from 17.0 to 31.9 with increase in sintering temperature from 1100 to 1400$^o$C. Similarly Ding et al. observed [48] increase in f from 11.2 to 33.4% with increase in temperature from 1400-1550$^o$C. With increase of temperature, the diffusion rate of oxygen toward SiC through $SiO_2$ film is accelerated in the early stage of the sintering so that more oxygen can further react with SiC to form $SiO_2$. Furthermore, the higher sintering temperature can speed up the viscous flow of oxidation derived $SiO_2$ [58]. Liu et al. [62] noticed with increase in graphite content from 0.25 to 0.6 (weight fraction) oxidation degree sharply increased from 30 to 49 % keeping the other processing parameter constant for cordierite bonded porous SiC ceramics. Oxidation degree was also found to be influenced by the particle size of the pore former. With increase of size of the pore former from 5 to 20 μm oxidation degree was found to reduce from 30 to 26.7%. It is proved by several authors that the oxidation degree of SiC is almost independent on the amount of pore former but it strongly depends on the particle size of SiC [46].

Eom et al. observed 2.3 mass% of $SiO_2$ on oxidation of 65 μm- SiC at 1550°C for 2 h, whereas the oxidation of 0.5 μm- SiC under the same conditions resulted in 48.1 mass % of $SiO_2$ [71]. In mullite bonded porous SiC ceramics prepared by infiltration route at 1500°C the % SiC oxidation degree was reduced from 65 to 7 % with increase of particle size from 4.47 to 99 μm [96]. A similar trend was also observed for samples prepared at 1300°C, where the % SiC oxidation degree decreased from 40 to 3% with increase of particle size from 4.47 to 99 μm.

For silica bonded SiC Ceramics the value of f varied from 12.2 to 13.06 for variation of fraction of pore former from 0.14 to 0.38 [84]. Mullite bonded SiC ceramics showed variation of f from 28-36.76 for variation of fraction of pore former from 0.15 to 0.51 [90]. Similarly with variation of fraction of pore former from 0.23 to 0.76 the cordierite bonded porous SiC ceramics showed variation of f from 22 to 39 [91]. It was observed that sample showed no significant changes in f when the pore former volume fraction was not very high. It is therefore likely that when the amount of pore former was not very high, the pore or void space that were created by burning of sacrificial pore former were not able to influence the process of SiC oxidation significantly, and consequently the % SiC oxidation degree showed no significant changes. But when the pore former amount was significantly higher, the pores or void spaces created by the pore formers were also higher which created higher surface area for SiC particles for oxidation and hence f was increased. Quanli et al. [149] also observed an increase in weight and rate constant and decrease of oxidation activation energy with decrease of particle size of SiC powders. In case of MBSC ceramics, decrease in f was observed with increase in amount of alumina in the starting powder mixture. This was because the coverage of surfaces of SiC particles by some fine alumina powders leading to the reduction in the surface area and thus f was reduced [48]. Same was also observed during formation of CBSC ceramics, where the oxidation degree of SiC was found to decrease from 48.4 to 42.5% with increase in weight fraction of $Al_2O_3$ and MgO from 0.1 to 0.3 [62]. It was noticed that the oxidation degree of SiC increases significantly with addition of $Y_2O_3$, $CeO_2$ and alkaline earth metal oxides [63,66]. This was due to the formation of glass of various compositions at low temperature. Ding et al. noticed [51] an increase of % oxidation degree of SiC from 24 to 35% for MBSC ceramics prepared with 1.5 wt % $Y_2O_3$ at 1500°C. With increase of oxidation degree amount of cristobalite formation increased and porosity decreased and hence mechanical properties improved to some extent.

### 3.5 Mechanical Properties of OBSC Ceramics

The mechanical strength of porous ceramics depends strongly on porosity and the microstructure. Therefore, the factors controlling the porosity are indirectly controlling the mechanical strength. For the porous SiC ceramics the factors affecting the strength includes the grain size, bonding necks between particles, bond phases, porosity, pore size distribution, pore shapes and flaws. The main parameters are the porosity and the bonding necks. The porosity depends on sintering temperature, forming pressure, content of pore former, etc., while bonding necks could be reflected from the densification of porous SiC ceramics. Table 1 shows that the flexural strength of oxide bonded porous SiC ceramics decreases with increase of porosity irrespective of the type of bond phase.

According to the minimum solid area (MSA) model [150], the strength of a porous material is related to its porosity by the expression:

$$\sigma = \sigma_o \exp(-bP) \quad (10)$$

where $\sigma$ is the strength of a material of porosity P, $\sigma_o$ is the strength of the completely dense material and b is a constant that depends on the shape and alignment of the pores. For the OBSC ceramics, the relation between strength and porosity of the ceramics sintered at a given temperature fits well with the Eq. (1) [47,48,50]. Strength decayed exponentially with increase in porosity as shown in Fig . 6. By fitting equation 1 with the plot of flexural strength vs. porosity, the values of $\sigma_o$ and b are obtained. The value of $\sigma_o$ and b obtained by different authors for oxide bonded porous SiC ceramics are summarized in Table 2.

For oxide bonded porous SiC ceramics with different oxide bond phases, different values for b could be estimated from the strength-porosity relationship. She et al. obtained the value of b = 6.5 to 7.1 for $SiO_2$-bonded porous SiC ceramic materials with porosity varying between 28 and 41 vol% [47]. Chun et al. reported still higher

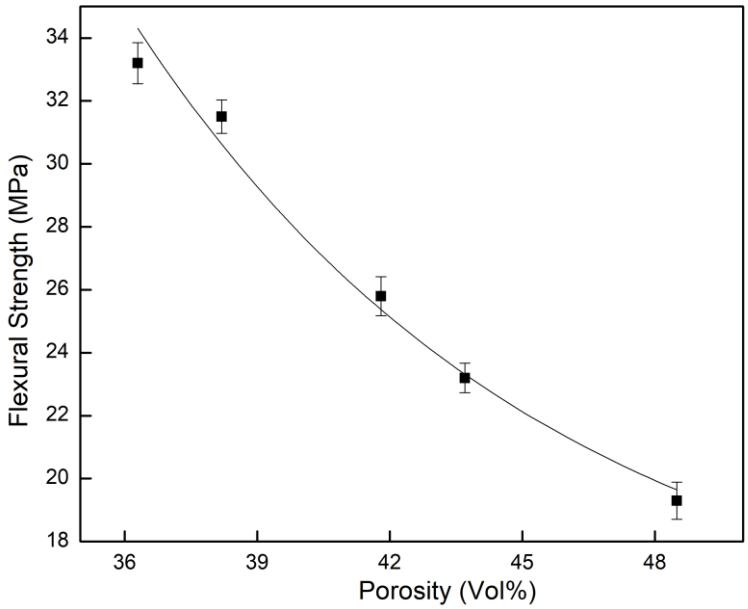


**Fig. 6. Plot of strength vs. porosity for mullite bonded porous SiC ceramics [87]**

value of b = 7.5 to 8.0 for the same material with porosity ranged from 19 to 77 vol.% [50]. Cordierite bonded porous SiC ceramics of porosity varying in the range of 28 to 60 vol% exhibited a value of b = 4.8 [55]. She et al. changed the porosity of the MBSC by varying the green density through the employment of different die pressing pressure, keeping the composition and sintering temperature and other processing parameter same and they reported value of b = 4.36, $\sigma_o$ = 190 MPa [48]. The cordierite bonded porous SiC ceramics prepared by conventional powder mixing method showed $\sigma_0$ =132 MPa and *b*=3.1 [82]. Bai et al. reported *b*=8.16 and $\sigma_0$ =1237.04 MPa for cordierite-mullite bonded porous SiC ceramics [80]. Liu *et al.* reported $\sigma_0$ =501 MPa and b=6.97 for cordierite bonded porous SiC ceramics prepared using 10 µm graphite powders as pore former [62]. Literature review indicated that processing conditions have a great impact on *b* and $\sigma_0$ values of final porous SiC ceramics. The values of *b* were reported to be 6 and 9 for cubic and rhombic stacking respectively [151]. The results of Table 2 indicated that the exponential factor 'b' did not change significantly with sintering temperature and oxide systems and the pore shape remained predominantly cylindrical in the final ceramics sintered at different temperatures. The results also indicated that OBSC ceramics followed the established strength-porosity dependence model and it is possible to alter their porosities to obtain desired level of strength values.

The Young's modulus is theoretically predicted by a relationship similar to the expression given in Eq. (1) [152]

$$E = E_o \exp(-bP) \quad (11)$$

where E is the Young's modulus of a material of porosity P, $E_o$ is the Young's modulus of the completely dense material and b is a constant that depends on the shape and stacking of the pores. By using the value of b obtained from Eq. 1, phase compositions of the sintered ceramics and the values of Young's moduli of the phases for a particular porosity level, the $E_o$ values of the sintered ceramics can be approximated by the rule of mixture. The Young's modulus ($E'_o$) of a completely dense ceramic material can be approximated by the rule of mixture [153]

$$E'_o = E'_1V_1 + E'_2V_2 + E'_3V_3 + \quad (12)$$

where $E'_1$, $E'_2$, $E'_3$,…… are the Young's modulus of the different constituent phases 1, 2, 3, …. of the dense ceramics and $V_1$,$V_2$,$V_3$,…… are their respective fractional volume. The $E'_o$ value were estimated using the values of Young's moduli of SiC [450 GPa], mullite [150 GPa], cordierite [70 GPa], cristobalite [72 GPa] glassy phase [72 GPa] [153-157] and their corresponding amount determined from X-ray and chemical analyses.

**Table 2. Porosity, flexural strength, b (the empirical constant) and $\sigma_o$ (the strength of corresponding non porous structure) of oxide-bonded porous SiC ceramics**

| Ref. | Type of bond phase | $\sigma_o$(MPa) | b | Porosity (Vol.%) | Strength (MPa) |
|---|---|---|---|---|---|
| 47 | silica | - | 6.54 - 7.08 | 41-28 | 100-185 |
| 48 | silica | 190 | 4.36 | 28-45 | 52-26 |
| 50 | Silica | - | 7.95 | 40 | 65 |
| 55 | SiC-mullite composite | 213.4 | 4.8 | 27.6-59.6 | 9.3-54.6 |
| 58 | mullite | - | - | 30-42 | 5-23 |
| 62 | cordierite | 501 | 6.97 | 66-28 | 3-70.3 |
| 71 | mullite | 167 | 4.89 | 35-42 | 13-38 |
| 78 | Mullite | 140 | 3.74 | 33-47 | 24-41 |
| 80 | Mullite-cordierite | 1237 | 8.16 | 37-53 | 15.6-55.4 |
| 82 | Cordierite | 132 | 3.1 | 22-45 | 30.9-65 |
| 88 | mullite | 181 | 4.6 | 36-49 | 19-33 |
| 90 | Mullite | 192 | 5.79 | 33-54 | 10-34 |
| 91 | Cordierite | 270 | 5.13 | 31-69 | 6-54 |
| 93 | Cordierite- silica | 195 | 5.05 | 30-36 | 13-38 |

To reduce sintering temperature and increase mechanical strength, various oxide additives along with alumina was added. The MBSC ceramics prepared from 20 µm SiC powder using $Y_2O_3$ and $Al_2O_3$ as additives resulted a flexural strength of 28 MPa at 44 vol% porosity and without $Y_2O_3$ addition resulted 24 MPa at 43 vol% porosity [54]. The addition of 4 wt% of alkaline earth metal oxides (SrO) found to improve mechanical strength of MBSC ceramics from 9 MPa at 49% poroity to 44 MPa at 46% porosity [66]. Mullite-bonded porous SiC ($d_{50}$=65 µm) ceramics prepared at 1500°C using 47.3 wt% $Al(OH)_3$ powder showed flexural strength of 14 MPa at 47 vol% porosity [69]. Significant improvement of flexural strength was obtained with addition of submicron SiC powder with coarse SiC powder [72]. Ebrahimpour et al. reported 30% enhancement of mechanical strength on replacement a portion of alumina powder by sol-gel alumina precursor due to increase of homogeneity. Depending on the processing parameters the reported flexural strength values of mullite bonded porous SiC ceramics using alumina powder as additives were 9.8 MPa at 50 vol% porosity, 24 MPa at 43 vol% porosity, 39 MPa at 36 vol% porosity and 45.49 MPa at 29.54 vol% porosity [53-54, 57]. The cordierite-bonded porous ceramics prepared from powder mixture of α-SiC ($d_{50}$ 10 µm), α-$Al_2O_3$, MgO and graphite (as pore former) by reaction bonding technique showed variation in flexural strength of ~70-3 MPa with variation of porosities ~28-65.6 vol% in final SiC ceramics[62]. With the increase of weight fraction of MgO+$Al_2O_3$ mixture from 0.2 to 0.3, the final SiC ceramics prepared at 1350°C showed a decrease in flexural strength due to formation of more Mg-Al-Si-O glass which made ceramics more fragile due to brittle nature. With addition of $CeO_2$ in the system an improvement of strength was obtained due formation of increased amount of cordierite phase with lesser amount of spinel phase [63]. The CBSC ceramics prepared by infiltration of cordierite precursor sol into powder compact of SiC ($d_{50}$=22 µm) sintered at 1400°C showed flexural strength of 38.3 MPa at 30.6 vol.% [93-94] . Li *et al.* recommended oxide bonded porous SiC as suitable candidate for hot gas filtration application as support material. They studied the effect of the moulding pressures, SiC particle sizes and oxide bond phase contents on mechanical strength of porous SiC ceramics [71].

## 3.6 Gas Permeation Behaviour

The gas permeability behaviour of the porous SiC ceramics can be well explained by Forchheimer's equation, the parabolic dependence of pressure drop ($\Delta P$) through a flat medium with the resulting face velocity ($v_s$) of the fluid [158]:

$$\frac{\Delta P}{L} = \frac{\mu}{k_1} v_s + \frac{\rho}{k_2} v_s^2 \qquad (13)$$

For compressible flow of gases and vapors, $\Delta P$ can be calculated from:

$$\Delta P = \frac{P_i^2 - P_o^2}{2P} \qquad (14)$$

in which $P_i$ and $P_o$ are absolute fluid pressures at the entrance and exit of the medium [Pa], L is the medium length or thickness(mm), $\mu$ is the

fluid viscosity [Pa.s] and $\rho$ is the fluid density [kg $m^{-3}$].

The terms $k_1$ and $k_2$ are the Darcian and non-Darcian permeability coefficients or constants, in reference to Darcy's law, which established a linear dependence between pressure drop and fluid velocity [159-161]. The permeability parameters obtained for the porous OBSC ceramics are presented in Table 3. Ding et al. [110] obtained variations in Darcian and non-Darcian permeability from 8.5 – 9.9 x $10^{-13}$ $m^2$ and 1.4 – 3.5 x $10^{-6}$ m respectively for a variation in porosity in a narrow range of 56-61.5% for MBSC ceramics [110]. Liu et al. [69] measured the permeability parameters of cordierite bonded porous SiC ceramics at two porosity levels, viz. 39 and 53% and obtained the Darcian permeability 0.71 x $10^{-13}$ and 0.88 x $10^{-13}$ $m^2$ respectively with the nearly same non-Darcian permeability ~0.02 x $10^{-6}$ m. The permeability behaviour of porous SiC ceramics was also compared with that of porous oxide ceramics [162]. From permeability studies it is observed that the sintering temperature and amount of pore former affect the permeability extremely by varying the texture of porous ceramics such as the open porosity, pore size distribution, and tortuosity of pore channels. Darcian and Non-Darcian permeability was found to increase with increase in amount of pore former during the fabrication of porous ceramics. At room temperature SBSC, MBSC and CBSC ceramics with porosity ~56% showed pressure drop of 12500, 5600 and 3000 Pa respectively at 0.05 m $s^{-1}$ face velocity [84,90-91].

## 3.7 Particle Filtration Behaviour Studies

The applicability of ceramic filter as hot gas filter depends on the filtration performance, permeability, durability, etc. in actual hot gas filtration condition [101-110]. In most of the previous studies dust filtration were carried out with commercial SiC ceramic candle filters in advanced power generation process [16-21]. Filtration performance in terms of collection efficiency and pressure drop of coupon size samples are also evaluated using the laboratory test set up to filter nano aerosol particles [105-110]. Very few studies are reported in literature on evaluation of filtration performance of the ceramic filter using laboratory made test set up to filter coal fly ash particles in actual power generation conditions [101-104]. The particle collection efficiency of a ceramic filter was determined by measuring the particle number concentration with an aerodynamic particle sizer. The particle are captured by the porous ceramics expresses their particle filtration efficiency. The overall efficiency was determined from the total particle mass concentration at the inlet and the outlet:

$$E_{overall} = \frac{C_{inlet} - C_{outlet}}{C_{inlet}} \quad (15)$$

Choi et al. measured the particle filtration efficiency of ceramic filters fabricated with SiC powders of various sizes (10–200 μm) [106]. Fly ash powder was used as test particles and filtration velocity was 1 m/min. The samples prepared with SiC 25 and 50 μm powders exhibited excellent collection efficiencies for particles larger than 1 μm. But the samples made with SiC10, SiC100 and SiC200 powders had low collection efficiencies due to the formation of pinholes and cracks and their inhomogeneity. The $E_{overall}$ of the samples of MBSC ceramics with porosity ~ 46.0% and 56%, was found to be >99% [90] and the CBSC with porosity ~ 62% exhibited the $E_{overall}$ 99% where NaCl nanoparticles were used as test particles [91]. Woo et al. fabricated SiC ceramic candle (500 mm long, 60 mm OD and 40 mm ID) from SiC powder of $d_{50}$ =180 μm using clay and other additives and filtration layer was developed by SiC powder of $d_{50}$ =14μm followed by sintering at 1400°C. The particle filtration efficiency and pressure drop of the candle filter was evaluated using laboratory made test set up. They used fly ash of $d_{50}$ = 5 μm as test particles and kept face velocity 5-9 cm $s^{-1}$. The pressure drop was found to increase with decrease of porosity, increase of face velocity and dust loading. They obtained variation of pressure drop between 6000-700 Pa at face velocity 0.07m/s. and ~100% filtration efficiency [101,102].

## 3.8 Thermal Shock and Oxidation Resistance Properties

Using the water quenching technique, the thermal shock behavior of the porous OBSC ceramics was evaluated as a function of quenching temperature, quenching cycles and specimen thickness. Thermal shock resistant of ceramic materials depend on flexural strength, elastic modulus, thermal expansion co-efficient, Poisson's ratio, shape of the samples, thermal conductivity, diffusivity, or emissivity, etc. [163-164]. The unified theory of fracture initiation and crack propagation [164] suggests that the

**Table 3. Permeability parameters of oxide bonded porous SiC ceramics**

| Material Characteristics | | Permeability parameters | | | | | [Ref.] |
|---|---|---|---|---|---|---|---|
| **Bond type** | **Porosity, P (%)** | **Flexural Strength (MPa)** | **Darcian permeability constant ($k_1$, $m^2$)** | **Non-Darcian permeability constant (k, m)** | **Pressure drop (Pa), (porosity)** | **Particle filtration efficiency (%)** | |
| Cordierite | 39 –53 | 11.1 -30 | 0.71-0.88 x $10^{-13}$ | 0.02 -0.02x $10^{-6}$ | - | - | 63 |
| Mullite | 25-62 | 3-24(at P 37-43.4 %) | 0-10 x $10^{-13}$ | 0-3.5 x $10^{-6}$ | - | - | 57 |
| Silica | 35.6 –56.4 | 5.4-29.5 | 1.64 -18.4 x $10^{-13}$ | 3.19-52.3 x $10^{-8}$ | 27,000 ( 46% ) and 5000 ( 56%) | - | 84 |
| Mullite | 29-55 | 9-34 | 1.21 × $10^{-13}$ to 1.60 × $10^{-12}$ | 5.8-29.5 × $10^{-8}$ | 15,000 at P 46% and 5700 at P 56% | 99.9 (at P 46-56%) | 90 |
| Cordierite | 30-55 | 14-54 | 0.8 -27 × $10^{-13}$ | 5.8-29.5× $10^{-8}$ | 4200 at P 46% and 3700 at P 56% | 96.7-99.9 (at P 68-62%) | 91 |
| Oxide | 21.2-40.4 | - | - | - | 490-88259 | 99% (particle size > 1 μm | 79 |
| oxide | 28.7-35.8 | 20 | - | - | 200-3000(without dust) 900-7500(with dust loading | 99.9 | 101 |
| glass | 32-64.7 | | 1.45-6.53× $10^{-12}$ | | | | 81 |
| SiC | 68-75 | | 0.13-0.82× $10^{-12}$ | - | - | - | 19 |
| LPS-SiC | 45-57 | 15-27 | 0.4-1.1× $10^{-12}$ | - | - | - | 20 |
| LPS-SiC | 86 | 16.6 (compressive str.) | 2.3-10 × $10^{-11}$ | | | | 21 |

damage by thermal shock depends on the degree of resistant to nucleating fracture. Li et al. suggested that the strength of SiC based ceramic composite decreases due to intrinsic brittle nature and sensitivity to crack after thermal shock [165]. Thermal shock analysis of oxide bonded porous SiC ceramics [47,52,54] showed a gradual decrease in flexural strength with increase in temperature gradient and thickness of the sample due to formation of cracks. This was interpreted that when the quenching temperature was > 200$^{o}$C, the tensile thermal stress caused crack formation in weaker necks which led to decrease in the load-bearing area and consequently in the fracture strength. With further increase in the quenching temperature and thus in the thermal stress, more and more necks were cracked. As a result, the measured strength decreased gradually with quenching temperature [52,54]. However, cracks were arrested at neck region during thermal shock analysis of SiC ceramics because of porous nature of materials which did not allow the damages been propagated properly and the ceramics reported to have excellent thermal resistance properties [52]. Moreover it was found that the fracture strength of the quenched specimens was not affected by the increase of the quenching cycles. Thermal shock resistance test of SiC composite also showed decrease of strength with quenching temperature up to certain temperature but with further increase of quenching temperature, a slow gain in strength was noticed which was explained by healing of some cracks [166] by oxidation derived silica glass. OBSC ceramics are having excellent oxidation resistance properties, due to the presence of $SiO_2$ layer on the surface of every SiC particles. She et al. observed only a weight increase ~ 0.5 %, on oxidizing OBSC ceramics in air at 1000$^{o}$C for 50 h [49]. The thermal shock resistance in combination with excellent oxidation resistance properties suggests a potential advantage of porous SiC ceramics for several industrial applications.

### 3.9 Other Application Areas

Porous silicon carbide (SiC) ceramic filters are commercially used for the combustion gas cleaning including IGCC and PFBC systems to clean combustion gas. SiC filters are also found suitable for High-Efficiency Particulate Air (HEPA) and Ultra-Low Penetration Air (ULPA) filters to provide extremely high collection efficiency of submicron airborne particles that are present in radioactive, biohazardous and highly toxic aerosols [167]. Porous SiC ceramic is becoming a potential microwave absorbing material because it has not only excellent microwave-absorbing property but also high mechanical strength and interconnected holes connected to the external. Additionally, porous ceramics have high thermal resistance and low volumetric heat capacity due to high porosity, low density and low thermal conductivity coefficient. Very recently porous SiC ceramics are used as super thermal insulation materials, energy conversion and environmental treatment technologies, for lithium polysulfide retention in Li–S batteries, for simultaneous removal of PM and volatile organic compounds, etc [168-170]. There are large numbers of areas where oxide bonded porous SiC ceramics could be used. Therefore constant efforts are going on the development of porous SiC ceramics for various industrial applications [171-172]. New mechanisms are required to balance properties of porous SiC ceramics processed by oxide bonding method for various industrial applications.

## 4. CONCLUSIONS

Large numbers of articles are reported on the development of porous SiC ceramics and their application, this review mainly focuses on the processing and properties of porous SiC ceramics processed by oxide bonding method. This paper highlighted the synthesis of porous SiC ceramics in air at low sintering temperature between ~ 900-1600°C where different secondary oxide bond phases (Mullite, Yttrium aluminium garnet, Cordierite, glass, frit, silica, etc) bonded the SiC particles. The oxidation bonding technique involves several advantages includes low processing temperature, cost effectiveness, easy control over the porosity, pore sizes and distribution of pores, with superior resistance to oxidation, etc. By selecting the type and amount of pore former, sintering temperature, size of the starting SiC powder, the porosity, pore size distribution and pore morphology can be controlled in the resultant SiC ceramics. Literature survey indicated that there are many issues on processing of porous SiC ceramics by oxide bonding method which need to be studied in detail that includes (1) the development of more cost-effective processing with homogeneous distribution of bond phase, narrow pore size distribution using low cost raw materials (2) investigate corrosion resistance and thermal shock resistance properties of the resulted porous ceramics (3) investigate other

important properties such as air permeability and particle filtration efficiency of the porous SiC ceramics (4) optimization of the processing parameters based on the desired required properties for specific application (5) further development of permeable filtration layer on the porous SiC support for further air filtration applications (6) development of further coating layer on the porous ceramic by some additives which can acts as the catalyst and adsorb some effluent gaseous. Therefore processing oxide bonded porous SiC ceramics with homogeneous formation of oxide bond phase along with full knowledge of air permeation, particle filtration, thermal and chemical shock resistance behaviour in real condition is essential. The processing of porous ceramics by oxidation bonding technique has been continuously improving to meet the requirement of microstructure, pore characteristics and properties as per the need of application areas. Further work should also be directed to explore new possible application areas of oxide bonded porous SiC ceramics.

## ACKNOWLEDGEMENT

The authors would like to thank SERB, Department of Science and Technology, Government of India (GAP-0261) for financial support.

## COMPETING INTERESTS

Authors have declared that no competing interests exist.

## REFERENCES

1. Ledoux MJ, Hanzer S, Huu CP, Guille J, Desaneaux MP. New synthesis and uses of high specific surface SiC as a catalytic support. J Catal. 1988;114(1):176-185.
2. Keller N, Huu CP, Roy S, Ledoux MJ, Estournes C, Guille J. `Surface area SiC for use as a heterogeneous catalyst support. J Mater Sci. 1999;34(13):3189-3202.
3. Huu CP, Bouchy C, Dintzer T, Ehret G, Estourness C, Ledoux MJ. High surface area silicon carbide doped with zirconium for use as catalyst support: preparation, characterization and catalytic application. Appl Catal. 1999;180(1-2):385-397.
4. Alvin MA. Impact of char and ash fines on porous ceramic filter life. Fuel process Tech. 1998;56(1-2):143-168.
5. Monnink H, Boven AJV, Peels HO, Tigchelaar I, Kam PJ, Crijns HJ, Oeveren WV. Silicon-carbide coated coronary stents have low platelet and leukocyte adhesion during platelet activation. J Investig Med. 1999;47(6):304-310.
6. Santavirta M, Takagi L, Nordsletten A, Anttila R, Lappalainen YT, Konttinen. Biocompatibility of silicon carbide in colony formation test in vitro. Arch Orthop Trauma Surg. 1998;118(1-2):89-91.
7. Gonzalez JP, Serra S, Chiussi S, Leon B, Amor MP, Fernandez JM, Lopez ARA, Feria FMV. New biomorphic SiC ceramics coated with bioactive glass for biomedical applications. Biomaterials. 2003;24(26): 4827-4832.
8. Gonzalez JP, Borrajo J, Serra S, Chiussi B, Leon J, Fernandez JM, Feria FMV, Lopez ARA, Carlos AD, Munoz FM, Lopez M, Singh M. A new generation of bio-derived ceramic materials for medical applications. J Biomed Mater Res. 2009;88:807-813.
9. Rosenbloom AJ, Sipe, DM, Shishkin Y, Ke Y, Devaty RP, Choyke WJ. Nanoporous SiC: a candidate semi-permeable material for biomedical applications. Biomed Microdevices. 2004;6(4):261-267.
10. Yu HS. Optimization of HEPA filter design. Proceedings of Institute of Environmental Sciences.1993;37(6):35-43.
11. Department of Energy Office of Transportation Materials. Light weight materials for transportation ORNL/ATD-75. Available from National Technical Information Service. US Department of Commerce. 5285 Port Royal Rd. Springfied; 1995.
12. Wen ZX, Liang JD, Hong TS, Microwave absorbing property of SiC reticulated porous ceramics. J Inorg Mater. 2002; 17(6):1152-1156.
13. Wei CG, Ridge TNO. Method for forming fibrous silicon carbide insulating material. US Pat 4481179; 1984.
14. Vonsivici A, Reed GT, Evans AG. β-SiC on insulator wave guide structures for modulators and sensor systems. Mat Sci Semicon Proc. 2000;3(5-6):367-382.
15. Wei CG, Ridge TNO. Method for forming fibrous silicon carbide insulating material. US Pat 4481179; 1984.
16. Schulz K, Walch A, Freude E, Durst M. Improved ceramic filter candles for hot gas cleaning in high temperature gas cleaning. Institut Fur Mechanische

Verfahrenstestechnik und Mechanik der Universitat Karlsruhe. Kalsruhe. Germany; 1996;835-845.
17. Newby RA, Lippert TE, Alvin MA, Burck GJ, Sanjana ZN. Status of westing house hot gas filters for coal and biomass power systems. J Eng Gas Turbines Power. 1999;121:401-408.
18. Yu HS. Optimization of HEPA filter design. Proceedings of Institute of Environmental Sciences. 1993;37(6):35-43.
19. Lücke T, Fissan H. The prediction of filtration performance of high efficiency gas filter elements. Chem Eng Sci. 1996; 51(8):1199-1208.
20. Stringer J, Leitch AJ. Ceramic candle filter performance at the gremethopre (UK) pressurized fluidized bed combustor. J Eng Gas Turbines Power. 1992;114():371-379.
21. Judkins RR. A review of the efficacy of silicon carbide hot gas filters in coal gasification and pressurized fluidized bed combustion. Fuel and Energy Abstracts. 1997;38(3):182.
22. Pastila PH, Helanti V, Nikkila AP, Mantyla TA. Effect of crystallization on creep of clay bonded SiC filters. Ceram Eng Sci Proc. 1998;19:3744.
23. Lee KS, Han IS, Seo DW, Woo SK. Strength degradation of silicon carbide hot gas in simulated PFBC condition. Key Engineering materials.2005;287:495.
24. Pastila P, Helanti V, Nikkila AP, Mantyla T. Environmental effects on microstructure and strength of SiC based hot gas filters. J Eur Ceram Soc. 2001;21(9):1261-1268.
25. Kim SH, Kim YW, Yun JY, Kim HD. Fabrication of porous SiC ceramics by partial sintering and their properties. J Kor Ceram Soc. 2004;41:541-546.
26. Sigl LS, Kleebe HJ. Core rim structure of liquid phase sintered silicon carbide. J Am Ceram Soc. 1993;76(3):773-776.
27. Studart AR, Gonzenbach UT, Tervoort E, Gauckler LJ, Processing routes to macroporous ceramics: A review. J Am Ceram Soc. 2006;89:1771–1789.
28. Kim YW, Kim SH, Song IH, Kim HD, Park CB. Fabrication of open-cell microcellular silicon carbide ceramics by carbothermal reduction. J Am Ceram Soc. 2005;88(10): 2949-2951.
29. Simonenko EP, Simonenko NP, Shembel NL, Simonov-Emel'yanov ID, Sevastyanov VG, Kuznetsov NT. Polymer technology of porous SiC ceramics using milled SiO2 fibers. Russ. J. Inorg. Chem. 2018;63(5): 574–582.
30. Sung IK, Yoon SB, Yu JS, Kim DP. Fabrication of macro porous SiC from templated preceramic polymers. Chem Commun. 2002;0(14):1480-1481.
31. Kumar BVM, Kim YW. Processing of polysiloxane-derived porous ceramics: A review. Sci Tecnol Adv Mater. 2010; 11(4):1-16.
32. Chae SH, Kim YW. Effect of inert filler addition on microstructure and strength of porous SiC ceramics. J Mater Sci. 2009; 44:1401-1406.
33. Jin J, Kim YW. Low temperature processing of highly porous silicon carbide ceramics with improved flexural strength. J Mater Sci. 2010;45:282-285.
34. Eom JH, Kim YW, Narisawa M. Processing of porous silicon carbide with toughened strut microstructure. J Ceram Soc Japan. 2010;118(5):380-383.
35. Eom H, Kim YW. Effect of additives on mechanical properties of macroporous silicon carbide ceremics. Met Mater Int. 2010;16(3):399-405
36. Kim YW, Jin YJ, Eom JH, Song IH. Engineering porosity in silicon carbide ceramics. J Mater Sci. 2010;45(10):2808-2815.
37. Lim KY, Kim YW, Song IH. Low temperature processing of porous SiC ceramics. Journal of Materials Science. 2013;48(5):1973-1979.
38. Greil P, Lifka T, Kaindl A. Biomorphic cellular ceramics from wood: I. Processing and microstructure. J Eur Ceram Soc. 1998;18(14):1961–1968.
39. Maddock AR, Harris AT. Biotemplated synthesis of novel porous SiC. Mat Lett. 2009;63(9-10):748-750.
40. Ota T, Takahashi M, Hibi T, Ozawa M, Suzuki H. Biomimetic process for producing SiC wood. J Am Ceram Soc. 1995;78(12):3409–3411.
41. Fukushima M, Zhou Y, Miyazaki H, Yoshizawa YI, Hirao K, Iwamoto Y, Yamazaki S, Nagano T. Microstructural characterization of porous silicon carbide membrane support with and without alumina additive. Journal of the American Ceramic Society. 2006;89(5):1523-1529.
42. Zhou Y, Fukushima M, Miyazaki H, Yoshizawa YI, Hirao K, Iwamoto Y, Sato K, Preparation and characterization of tubular porous silicon carbide membrane supports.

Journal of membrane science. 2011;369(1-2):112-118.
43. Huang Q, Jin Z. The high temperature oxidation behaviour of reaction-bonded silicon carbide. J Mater Proc Tech. 2001;110:142–145.
44. Zheng C, Yang Z, Zhang J, High temperature oxidation behaviour of reaction-bonded porous silicon carbide ceramics in dry oxygen. J Am Ceram Soc. 2010;93(7):2062-2067.
45. Zhu XW, Jiang DL, Tan SL. Preparation of silicon carbide reticulated porous ceramics. Mat Sci Eng. 2002;23(1-2):232-238.
46. She JH, Yang JF, Kondo N, Ohji T, Kanazaki S, Deng ZY. High strength porous silicon carbide ceramics by an oxidation-bonding technique. J Am Ceram Soc. 2002;85(11):2852-2854.
47. She J, Ohji T, Deng ZY. Thermal shock behaviour of porous silicon carbide ceramics. Journal of the American Ceramic Society. 2002;85(8):2125-2127.
48. She JH, Deng ZY, Doni JD, Ohji T. Oxidation bonding of porous silicon carbide ceramics. J. Mater. Sci. 2002;37(17):3615-3622.
49. She JH, Ohji T, Kanazaki S. Oxidation bonding of porous silicon carbide ceramics with synergic performance. J Euro Ceram Soc. 2003;24(2):331-334.
50. Chun YS, Kim YW. Processing and mechanical properties of porous silica-bonded silicon carbide ceramics. Met Mater Int. 2005;11(5):351-355.
51. Ding S, Zhu S, Zeng YP, Jiang D. Effect of $Y_2O_3$ addition on the properties of the reaction bonded porous SiC ceramics. Ceram Intl. 2006;32(4):461-466.
52. Ding S, Zhu S, Zeng YP, Jiang D. Thermal shock resistance of in situ reaction bonded porous silicon carbide ceramics. Mat Sci & Eng. 2006;425(1-2):326-329.
53. Ding S, Zhu S, Zeng YP, Jiang D. Fabrication of mullite bonded porous silicon carbide ceramics by in situ reaction bonding J Euro Ceram Soc. 2007;27(4):2095-2102.
54. Ding S, Zeng YP, Jiang D. Thermal shock behaviour of mullite-bonded porous silicon carbide ceramics with yttria addition. Phys D: applied Phys. 2007;40(7):2138-42.
55. Zhu S, Ding S, Xi H, Li Q, Wang R. Preparation and characterization of SiC/cordierite composite porous ceramics. Ceram Intl. 2007;33(1): 115-118.
56. Lee JS, Choi DM, Choi SC. Preparation and characterization of cordierite-bonded silicon carbide porous ceramics, in solid state phenomena. Trans Tech Publ. 2007;124:747-750.
57. Ding S, Zeng YP, Jiang D. Gas permeability behavior of mullite-bonded porous silicon carbide ceramics. Journal of Materials Science. 2007;42(17):7171-7175.
58. Ding S, Zeng YP, Jiang D. In situ reaction bonding of porous SiC ceramics. Mater Charac. 2008;59(2):140-143.
59. Bardhan N, Bhargava P, In situ reaction sintering of porous mullite bonded silicon carbide: Its mechanical behaviour and high temperature application. Ceram Eng Sci Proc. 2008;29(2):127-140.
60. Warrier KG, Kumar GMA, Ananthakumar S. Densification and mechanical properties of mullite-SiC nanocomposites synthesized through sol-gel coated precursors. Bulletin of Materials Science. 2001;24(2):191-195.
61. Eom JH, Kim YW. Effect of template size on microstructure and strength of porous silicon carbide ceramics. Journal of the Ceramic Society of Japan. 2008;116(10):1159-1163.
62. Liu S, Zeng YP, Jiang D. Fabrication and characterization of cordierite bonded porous silicon carbide ceramics. Ceram Int. 2009;35(2):597-602.
63. Liu S, Zeng YP, Jiang D. Effects of $CeO_2$ addition on the properties of cordierite-bonded porous SiC ceramics. J Euro Ceram Soc. 2009;29(9):1795-1802.
64. Chae SH, Kim YW, Song IH, Kim HD, Bae JS, Na SM, Kim SI. Low temperature processing and properties of porous frit-bonded SiC ceramics. Journal of the Korean Ceramic Society. 2009;46(5):488-492.
65. Liu S, Zeng YP, Jiang D. Effects of preheat treated aluminosilicate addition on the phase development, microstructure, and mechanical properties of mullitized porous OBSC ceramics. Int J Appl Ceram Technol. 2009;6(5):617–625.
66. Choi YH, Kim YW, Han IS, Woo SK. Effect of alkaline earth metal oxide addition on flexural strength of porous mullite bonded silicon carbide ceramics. J Mat Sci. 2010;45:6841-44.
67. Kumar BVM, Eom JH, Kim YW, Han IS, Woo SK. Effect of aluminum source on flexural strength of mullite bonded porous

silicon carbide ceramics. J Ceram Soc Jpn. 2010;118(1):13-18.
68. Feng LJ, Hong L, Bao LJ. Influence factors on the porosity and strength of SiC porous ceramic. J Inorg Mater. 2011;26:944-948.
69. Kumar BVM, Eom JH, Kim YW, Song IH, Kim HD. Effect of aluminium hydroxide content on porosity and strength of porous mullite-bonded silicon carbide Ceramics J Ceram Soc Jpn. 2011;119 (5):367-370.
70. Kumar VM, Lim KY, Kim YW. Influence of submicron SiC particle addition on porosity and flexural strength of porous self-bonded silicon carbide. Met Mater Int. 2011;17(3):435-440.
71. Li J, Lin H. Factors that influence the flexural strength of SiC based porous ceramics used for hot gas filter support. Journal of the European Ceramic Society. 2011;31(5):825-831.
72. Eom JH, Kim YW. Effect of initial α-phase content on microstructure and flexural strength of macroporous silicon carbide ceramics. Metals and Materials International. 2012;18(2):379-383.
73. Lim KY, Kim YW, Song IH. Porous sodium borate bonded SiC ceramics. Ceramics International. 2013;39(6):6827-6834.
74. Ebrahimpour O, Chaouki J, Dubois C. Diffusional effects for the oxidation of SiC powders in thermogravimetric analysis experiments. Journal of Materials Science. 2013;48(12):4396-4407.
75. Ebrahimpour O, Esmaeili B, Griffon L, Chaouki J, Dubois C, Novel fabrication route for porous silicon carbide ceramics through the combination of in situ polymerization and reaction bonding techniques. Journal of Applied Polymer Science. 2014;131:40425.
76. Ebrahimpour O, Dubois C, Chaouki J. Manufacturing process for in situ reaction-bonded porous SiC ceramics using a combination of graft polymerization and sol–gel approaches. Industrial & Engineering Chemistry Research. 2014;53(45):17604-17614.
77. Ebrahimpour O, Dubois C, Chaouki J. Fabrication of mullite-bonded porous SiC ceramics via a sol–gel assisted in situ reaction bonding. Journal of the European Ceramic Society. 2014;34(2):237-247.
78. Bai CY, Deng XY, Li JB, Jing YN, Jiang WK. Preparation and properties of mullite-bonded porous SiC ceramics using porous alumina as oxide. Materials Characterization. 2014;90:81-87.
79. Choi HJ, Kim JU, Kim SH, Lee MH. Preparation of granular ceramic filter and prediction of its collection efficiency. Aerosol Science and Technology. 2014; 48(10):1070-1079.
80. Bai CY, Deng XY, Li JB, Jing YN, Jiang WK, Liu ZM, Li Y. Fabrication and properties of cordierite–mullite bonded porous SiC ceramics. Ceramics International. 2014;40(4):6225-6231.
81. Wang B, Zhang H, Phuong HT, Jin F, Yang JF, Ishizaki K. Gas permeability and adsorbability of the glass bonded porous silicon carbide ceramics with controlled pore size. Ceramics International. 2015; 41(2):2279-2285.
82. Shi W, Liu B, Deng X, Li J, Yang Y. In-situ synthesis and properties of cordierite-bonded porous SiC membrane supports using diatomite as silicon source. Journal of the European Ceramic Society. 2016;36(14):3465-3472.
83. Yuan B, Wang G, Li H, Liu L, Liu Y, Shen Z. Fabrication and microstructure of porous SiC ceramics with $Al_2O_3$ and $CeO_2$ as sintering additives. Ceramics International. 2016;42(11):12613-12616.
84. Dey A, Kayal N, Innocentini MDM, Chacon WS, Coury JR, Chakrabarti OP. On evaluation of permeability parameters of oxide bonded porous SiC ceramics. Int. J. App Ceram Tech. 2013;10(6):1023–1033.
85. Dey A, Kayal N, Chakrabarti OP. Preparation of porous SiC ceramics by an infiltration technique. Ceramics International. 2011;37(1):223-225.
86. Dey A, Kayal N, Chakrabarti OP. Preparation of porous mullite bonded SiC ceramics by an infiltration technique. Journal of Materials Science. 2011; 46:5432-38.
87. Kayal N, Dey A, Chakrabarti OP. Incorporation of mullite as a bond phase into porous SiC by an infiltration technique. Materials Sci and Eng A. 2012;535:222-227.
88. Kayal N, Dey A, Chakrabarti OP. Synthesis of mullite bonded porous SiC ceramics by a liquid precursor infiltration method: Effect of sintering temperature on material and mechanical properties. Mater Sci and Eng A. 2012;556:789-795.
89. Baitalik S, Dey A, Chakrabarti OP, Kayal N. Effect of SiC particle size on the material and mechanical properties of mullite bonded porous SiC ceramics processed by

precursor sol infiltration technique. Ceram Silikaty. 2014;58(4):326-332.

90. Dey A, Caldato RF, Guerra VG, Innocentini MDM, Kayal N, Chakrabarti OP. Investigations on material and mechanical properties, air-permeation behaviour and filtration performance of mullite bonded porous SiC ceramics. Int J Appl Ceram Tech. 2014;11(5):804-814.
91. Dey A, Kayal N, Chakrabarti OP, Caldato RF, André CM, Innocentini MDM. Permeability and nanoparticle filtration assessment of cordierite bonded porous SiC ceramics. Indus and Eng Chem Res. 2013;52(51):18362−18372.
92. Baitalik S, Kayal N, Chakrabarti OP. Processing and properties of porous SiC ceramics prepared by YAG infiltration. Int J Appl Ceram Tech. 2017;14(4):652-664.
93. Baitalik S, Kayal N. Processing and properties of cordierite-silica bonded porous SiC ceramics. Ceram Int. 2017; 43(17):14683-14692.
94. Baitalik S, Dalui SK, Kayal N. Mechanical and microstructural properties of cordierite bonded porous SiC ceramics processed by infiltration technique: Influence of pore formers. J of Mat Sci. 2018;53(9):6350-6365.
95. Dey A, Kayal N, Molla AR, Chakrabarti OP. Investigation of thermal oxidation of $Al_2O_3$-coated SiC powder. Thermochim Acta. 2014;583:25-31.
96. Baitalik S, Chakrabarti OP, KayaL N. Fabrication of mullite bonded porous SiC ceramics via a sol-gel coated precursors. Trans. Ind. Ceram. Soc. 2015; 74(2):1-5.
97. Baitalik S, Kayal N, Chakrabarti OP. Properties of mullite bonded SiC ceramics from mullite precursor sol coated SiC powder and crystallization kinetics of mullite formation. Materials Res Innovations. 2016;20(2):99-105.
98. Baitalik S, Panigrahi D, Kayal N. Properties of porous SiC ceramics processed by gelation and consolidation of boehmite coated SiC suspensions. Trans Ind Ceram Soc. 2017;76(4):222-227.
99. Baitalik S, Kayal N. Dispersion of SiC powder suspension in mullite sol and influence on properties of sintered ceramics. Int J Appl Ceram Tech. 2018; 15(2):426-437.
100. Baitalik S, Molla AR, Kayal N. Investigation on oxide bonded porous SiC ceramics from SiC powder co-precipitated with yttrium aluminum garnet (YAG) sol and non-isothermal kinetics of oxide bond phase formation. Int J alloys and Compounds. 2018;767:302-314.
101. Woo SK, Lee KS, Hub IS, Seo DW, Park YO. Role of porosity in dust cleaning of silicon carbide ceramic filters. J Ceram Soc Japan. 2001;109(9):742-747.
102. Lee KS, Woo SK, Han IS, Seo DW, Park SJ, Park YO. Filtering characteristics of porous SiC filter with high surface area. J Ceram Soc Jpn. 2002;110(7):656-661.
103. Choi JH, Keum SM, Chung JD. Operation of ceramic candle filter at high temperature of PFBC application. Korean J of Chem Eng. 1999;16(6):823-828.
104. Kim JH, Liang Y, Sakong KM, Choi JH, Bak YC. Temperature effect on the pressure drop across the cake of coal gasification ash formed on a ceramic filter. Powder Tech. 2008;181(1):67-73.
105. Freitas NL, Gonçalves JAS, Innocentini MDM, Coury JR. Development of a double-layered ceramic filter for aerosol filtration at high-temperatures: The filter collection efficiency. J Hazard Mat. 2006;136(3):747-56.
106. Choi HJ, Kim JU, Kim SH, Lee MH. Preparation of granular ceramic filter and prediction of its collection efficiency aerosol. Science and Technology. 2014; 48(10):1070–1079.
107. Chi H, Ji Z, Sun D, Cui L. Experimental investigation of dust deposit with in ceramic filter medium during filtration cleaning cycles. Chin J Chem Eng. 2013; 17:219–225.
108. Zhong Z, Xing W, Li X, Zhang F. Removal of organic aerosols from furnace flue gas by ceramic filters. Ind Eng Chem Res. 2013;52(15):5455–5461.
109. Innocentini MDM, Tanabe EH, Aguiar ML, Coury JR. Filtration of gases at high pressures: Permeation behavior of fiber based media used for natural gas cleaning. Chemical Engineering Science. 2012; 74:38–48.
110. Biasetto, Colombo P, Innocentini MDM, Mullens S. Gas permeability of microcellular ceramic foams. Ind & Eng Chem Res. 2007;46(10):3366.
111. Bakshi AK, Ghimire R, Sheridan E, Kuhn M. Treatment of produced water using SiC membrane filters. Ceramic Engineering and Science Proceedings. 2015;36(5): 91-98.

112. Hagen K. Ultra and microfiltration for dam water treatment, In Reports of the Rheinisch Westfaelischem Institut fuer wasserchemie und wasserteechnologie GmbH Muelheim Germany. 1996;16:131-142
113. Neufert R, Moeller M, Bakshi AK. Dead-end silicon carbide micro-filters for liquid filtration. Advances in Bioceramics and Porous Ceramics VI: Ceramic Engineering and Science Proceedings. 2013;34:115-126.
114. Bakshi AK, Ghimire R, Sheridan E, Kuhn M. Treatment of produced water using silicon carbide membrane filters. Ceramic Engineering and Science Proceedings. 2015;36(5):91.
115. Stobbe P, Hack U. Porous ceramic body and method for production thereof. US Pat 7699903 B2. 2010.
116. Fraga MC, Sanches S, Crespo JG, Pereira VJ. Assessment of a new silicon carbide tubular honeycomb membrane for treatment of olive mill wastewaters. Membranes. 2017;7(1):12.
117. Beni AH. Screening of microfiltration and ultrafiltration ceramic membranes for produced water treatment and testing of different cleaning methods. Thesis Master of Applied Science in Process Systems Engineering. University of Regina. Saskatchewan; 2014.
118. Mulatu MM. Silicon carbide based capillary membranes for gas separation and water treatment, Master Thesis Universidad Zaragoza European Master Erasmus Mundus Master in membrane engineering. Institus Euorpeen des Membrnaes. 2014.
119. Kim SC, Kim YW, Song IH. Processing and properties of glass-bonded silicon carbide membrane supports. J Eur Ceram Soc. 2017;37(4):1225-1232.
Kim SC, Yeom HJ, Kim YW, Song IH, Ha JH. Processing of alumina-coated glass-bonded silicon carbide membranes for oily wastewater treatment. Int J Appl Ceram Technol. 2017;14(4):692-702.
120. Das D, Baitalik S, Haldar B, Saha RN, Kayal N. Preparation and characterization of macroporous SiC ceramic membrane for treatment of waste water. J of Porous Materials. 2018; 25(4):1183-1193.
121. Jorgenson PJ, Wadsworth ME, Cutler IB. Oxidation of silicon carbide. J Am Ceram Soc. 1959;42(12):613-616.
122. Ervine G. Oxidation behaviour of silicon carbide. J Am Ceram Soc. 1958;41:347-352.
123. Zok F, Lange FF, Porter JR. Packing density of composite powder mixtures. J Am Ceram Soc. 1991;74(8):1880-85.
124. Lange FF, Atteraas L, Zok F, Porter JR. Deformation consolidation of metal powders containing steel inclusions. Acta Metall Mater. 1991;39(2)209-19.
125. Almarahle G. Production of silica refractory bricks from white sand. Am J Appl Sci. 2005;2(1):465-468.
126. Harako H, Akahori S. Process for producing silica brick. European Patent EP0544913 B1; 1995.
127. Aksay IA, Pask JA. Stable and metastable phase equillibria in the system $Al_2O_3$-$SiO_2$. J Am Ceram Soc. 1975;58(11-12):507-512.
128. Saruhan B, Albers W, Schneider H, Kaysser WA. Reaction and sintering mechanism of mullite in the systems cristobalite/ α-$Al_2O_3$. J Euro Ceram Soc. 1996;16(10):1075-1081.
129. Miao X. Porous mullite ceramics from natural topaz. Materials Letters. 1999; 38(3):167-172.
130. Lee JE, Kim JW, Jung YG, Jo CY, Paik U. Effects of precursor pH and sintering temperature on synthesizing and morphology of sol–gel processed mullite. Ceramics international. 2002;28(8):935-940.
131. Dey A, Kayal N, Innocentini MDM, Chakrabarti OP. Investigation on sacrificial pore former removal and mullite binder phase transformation in powder formulations used for preparation of
132. oxide bonded porous SiC ceramics. Ceram Int. 2017;43(12):9416–9423.
133. Milberg ME, Blair HD. Thermal expansion of cordierite. J Am Ceram Soc. 1977;60(7-8):372-373.
134. Sano S, Nagoya JP. Method for manufacture of low thermal expansion cordierite ceramics. US Patent 4495300. 1985.
135. Goren R, Gocmez H, Ozgur C. Synthesis of cordierite powder from talc,diatomite and alumina. Ceram Int. 2006;32(4):407–409.
136. Kumar S, Singh KK, Ramachandrarao P. Synthesis of cordierite from fly ash and its refractory properties. J Mater Sci Lett. 2000;19:1263–1265.

137. Kobayashi Y, Sumi K, Kato E. Preparation of dense cordierite ceramics from magnesium compounds and kaolinite without additives. Ceram Int. 2000; 26(7):739–743
138. Buaishi NME, Ćastvan IJ, Jokić B, Veljovic D´, Janaćković D, Petrović R. Crystallization behaviour and sintering of cordierite synthesized by an aqueous sol–gel route. Ceram Inter. 2012;38(3):1835–1841.
139. Yuritsin NS, Fokin VM, Kalinina AM, Filipovich VN. In Proceedings of the XVI International Congress on Glass. Bol Soc Esp Ceram Vid. 1992;31(5):21-26.
140. Muller R. The influence of grain size on the overall kinetics of surface-induced glass crystallization. J Thermal Anal. 1989; 35(3):823.
141. Mora ND, Ziemath EC, Zanotto ED. In Proceedings of the XVI International Congress on Glass. Bol Soc Esp Ceram Vid. 1992;31(5):117-118.
142. Mechnich P, Schneider H. Reaction bonding of mullite (RBM) in presence of scandia $Sc_2O_3$. J Euro Ceram Soc. 2008;28(2):473
143. Bondar IA, Galakhov FY. Phase equilibria in the system $Y_2O_3$-$Al_2O_3$-$SiO_2$. Bulletin of the Academy of Sciences of the USSR.1963;3(7):1321-1325.
144. Osborn EF, Muan A. Phase equilibrium diagrams of oxide systems. The American Ceramic Society; 1960.
145. Osborn EF, Muan A Phase equilibrium diagrams of oxide systems plate 1. The American Ceramic Society. Westerville; 1960.
146. Gnesin GG, Shipilova LA, Chernyshev LI, Loikovskii V, Prez A. Formation of highly porous ceramic based on silicon carbide. Power Metta Meta Ceram. 1994;33(5-6):262-267.
147. Wu S, Claussen N. Fabrication and properties of low-shrinkage reaction-bonded mullite. J Am Ceram Soc. 1991;74(10):2460–2463.
148. He J, Ponton CB. Oxidation of SiC powders for the preparation of SiC/mullite/alumina nanocomposites. J Mater Sci. 2008;43(12):4031–4041.
149. Quanli J, Haijun Z, Suping L, Xiaolin. Effect of particle size on oxidation of silicon carbide powders. J. Ceram Int. 2007; 33(2):309.
150. Rice RW. Comparison of stress concentration versus minimum solid area based mechanical property-porosity relations. J Mater Sci. 1993;28(8):2187-2190.
151. Knudsen FP. Dependence of mechanical strength of brittle crystalline specimens on porosity and grain size. J Am Ceram Soc. 1959;42(8):376-387.
152. Rice RW. Extension of the exponential porosity dependence of strength and elastic moduli. J Am Ceram Soc. 1976;59(11-12):536-537.
153. Voigt W. On the relationship between the two elastic constants of isotropic bodies. Ann Phys Chem. 1889;274(12):573-587.
154. Carnahan RW. Elastic properties of silicon carbide. J Am Ceram Soc. 1968;51(4):223-224.
155. Pastila P, Nikkila AP, Mantyla T, Curzio EL. Effect of thermal cycling to the strength and fracture of SiC-based candle filters. Ceram Eng Sci Porc. 2002;23(3):607–613.
156. Hayati EZ, Moradi OM, Kakroudi MG. Investigation the effect of sintering temperature on Young's modulus evaluation and thermal shock behavior of a cordierite–mullite based composite. Mater. Des. 2013;45(3):571–575.
157. Tsuzuki T, Mitamura N. Glass composition; European Patent 2 233 445 A1; 2010.
158. Noman R, Kalam MZ. Transition from laminar to non-Darcy flow of gases in porous media: In Advances in Core Evaluation: Accuracy and Precision in Reserves Estimation. 1990. 447–462.
159. Seguin D, Montillet A, Comiti J. Experimental characterization of flow regimes in various porous media–I: Limit of laminar flow regime. Chem Eng Sci. 199;853(21):3751–3761.
160. Seguin D, Montillet A, Comiti J, Huet F. Experimental characterization of flow regimes in various porous media–II: Transition to turbulent regime. Chem Eng Sci. 1998;53(22):3897–3909.
161. Hlushkou D, Tallarek U. Transition from creeping via viscous-inertial to turbulent flow in fixed beds. J Chromatogr A. 2006;1126(1-2):70–85.
162. Innocentini MDM, Pardo ARF, Menegazzo BA, Bittenocourt LRM, Rettore RP, Pandolfelli VC. Permeability of high alumina refractory castable based on various hydraulic binders. J Am Ceram Soc. 2002;85(6):1517-1521.
163. Kingery W. Factors Affecting Thermal Stress Resistance of Ceramic Materials. J Am Ceram Soc. 1955;38(1):3.

164. Hasselman D. Elastic Energy at Fracture and Surface Energy as Design Criteria for Thermal Shock. J Am Ceram Soc. 1963;46(11):535.
165. Li G, Chen H. Effect of Repeated Thermal Shock on Mechanical Properties of $ZrB_2$-SiC-BN Ceramic Composites. The Scientific World Journal. 2014;14-15:ID 419386.
166. Zhai F, Li S, Sun J, Yi Z. Microstructure, mechanical properties and thermal shock behavior of h-BN-SiC ceramic composites prepared by spark plasma sintering. Ceram Int. 2017;43(2):2413-2417.
167. Mitchell MA, Bergman W, Haslam J, Brown EP, Sawyer S, Beaulieu R, Althouse P, Mieke A. Ceramic HEPA filter program, 32nd Nuclear air cleaning conference, International society for nuclear air treatment technologies. CO, USA, June 17-19; 2012.
168. Xue Y, Xie J, He M, Liu M, Xu M, N Wei and Yan YM, Porous and high-strength graphitic carbon/SiC three-dimensional electrode for capacitive deionization and fuel cell applications. J. Mater. Chem. A. 2018;6:19210-19220.
169. Fen Li and Jijun Z, Three dimensional porous SiC for lithium polysulfide trapping, Phys. Chem. Chem. Phys. 2018;20: 4005—4011.
170. Li C, Zhang F, Shasha F, Wu H, Zhong Z, Xing W, SiC@TiO2/Pt Catalytic Membrane for Collaborative Removal of VOCs and Nanoparticles, Ind. Eng. Chem. Res. 2018;57:10564−10571.
171. Hanna SB, Awaad M, Ajiba NA, Saad EA, Characterization of Porous Alumino-Silicate Bonded SiC-Ceramics Prepared by Hand-Pressing and Extrusion Methods, Silicon. 2018;10:1961–1972.
172. Gu T, Chen F, Yuan H, Shen Q and Zhang L, Low temperature sintering of porous silicon carbide ceramics with $H_3PO_4$ as an additive. Solid State pheonomena, 2018; 281:311-315.



*Peer-review history:*
*The peer review history for this paper can be accessed here:*
*http://www.sciencedomain.org/review-history/27940*